Protein-templated metal nanoclusters for chemical sensing

Han-Wei Chu[1†], Girum Getachew Demissie[1†], Chih-Ching Huang[2] and Anisha Anand[3]*

[1]Department of Biomedical Sciences, College of Medicine, Chang Gung University, Taoyuan, Taiwan,
[2]Department of Bioscience and Biotechnology, National Taiwan Ocean University, Keelung, Taiwan,
[3]Department of Biomedical Engineering, Chang Gung University, Taoyuan, Taiwan

Metal nanoclusters (MNCs) possess unique optical properties, discrete energy levels, biocompatibility and photostability, making them pivotal photoluminescent probes in chemical sensing. While substantial work has addressed the synthesis, theoretical studies and applications of gold-, copper-, and silver-based MNCs, this review introduces fresh perspectives on how the nature and concentration of templates—particularly protein molecules—affect the optical properties, stability and sensing capabilities of MNCs. We delve into the merits of using protein templates for creating highly stable MNCs with tunable photoluminescence (PL), providing a detailed comparison with non-protein based systems. This review also unveils recent advancements in the photophysical characteristics and chemical sensing applications of protein-templated MNCs, setting it apart from previous reviews by focusing on cutting-edge innovations in template influence. Challenges and future prospects for protein-templated MNCs in chemical sensing are highlighted, marking critical pathways for upcoming research. This work not only integrates current knowledge but also identifies gaps and opportunities not covered extensively in earlier reviews, such as the nuanced effects of template variation on MNCs' functional properties.

KEYWORDS

metal nanoclusters, protein templates, precise control, tunable PL, chemical sensing

1 Introduction

Over the past decades, metal nanoclusters (MNCs) have captured significant interest across various scientific and technological disciplines due to their remarkable opto-electronic properties, high electron mobility, extended photoluminescence (PL) lifetimes and considerable diffusion lengths (Zare et al., 2021; Qiao et al., 2021; Jin et al., 2020; Lin et al., 2022; Wei et al., 2022). These clusters are characterized by a core-shell structure, with metal at the core and stabilizing ligands forming a protective shell that interacts covalently with the metal surface (Chen T. et al., 2022; Yang et al., 2020; Xiao et al., 2021; Lin et al., 2021a; Hu et al., 2022; Mathew et al., 2023). MNCs are crafted using diverse metal ions to create ligand-protected, quantum-sized clusters with cores smaller than 2 nm, exhibiting unique photophysical traits (Wei et al., 2022; Paulrajpillai et al., 2012; Thakran et al., 2021). The high surface-to-volume ratio (molecular-like) and quantum confinement effects endow MNCs with exceptional optical properties and catalytic activities (Li X. et al., 2021; Ebina et al., 2020; Kang and Zhu, 2019; Wang C C et al., 2016). The physicochemical properties of MNCs are intricately linked to the nature of the metal core and surface ligand chemistry, along with other environmental factors such as temperature, solvent and pH (Romeo et al., 2021; Qian et al., 2022; Chakraborty and Mukherjee, 2022). Crucially, the size of the metal

GRAPHICAL ABSTRACT
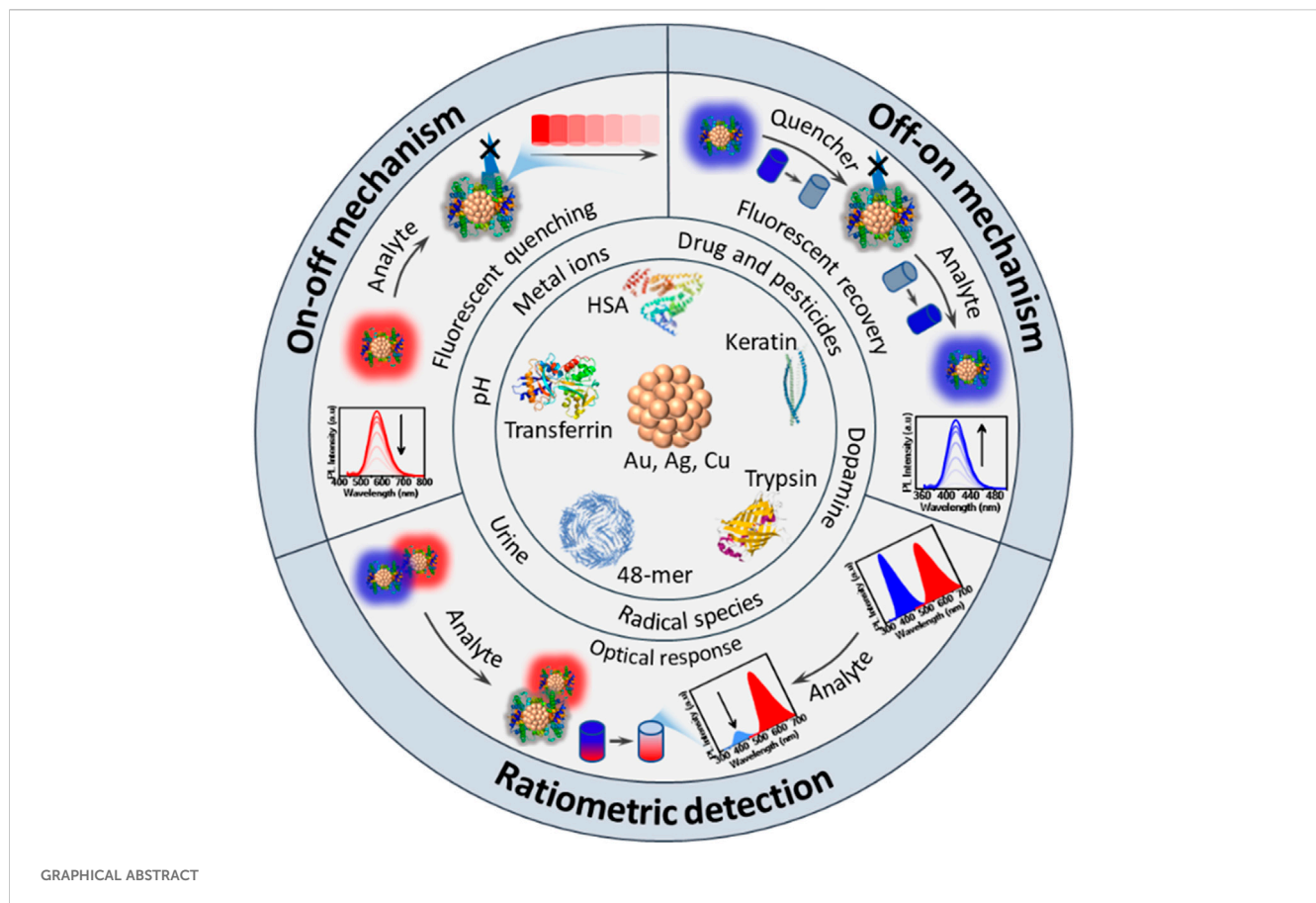
core and the chemistry of the surface ligands play pivotal roles in defining the PL properties and catalytic capabilities of MNCs. By varying the particle size, one can tune these PL properties due to the quantum confinement effect, potentially altering their characteristics and enhancing their performance across various applications. Particularly, the use of photoluminescent MNCs in chemical sensing is driven by their notable PL properties and prolonged PL lifetimes (Lin et al., 2022; Thakran et al., 2021; Lin et al., 2024).

MNC-based sensors fabricated from metals such as gold (Au), copper (Cu), silver (Ag) and platinum (Pt) have been widely recognized as excellent probes for photoluminescent sensing applications (Lin et al., 2021b; Shen et al., 2021; Fereja et al., 2021; Liu et al., 2020; Chang et al., 2021; Chen X. et al., 2020; Yen et al., 2022; Yu et al., 2017; Tseng et al., 2018; Jin et al., 2019). Numerous studies have investigated the role of surface ligands and ligand-metal interfaces in the performance of MNC-based chemical sensors (Matus and Häkkinen, 2023; Aparna et al., 2022; Nasrollahpour et al., 2023). Surface ligands play a critical role in enhancing the stability and selectivity of the sensors. Functional moieties on these surface ligand molecules form either strong covalent bonds or matrix encapsulations with the metal core, contributing to the sensor's long-term stability and improved selectivity toward specific substrates. Moreover, the surface chemistry of these ligands is essential for regulating the interaction between the analyte and the metal core, which directly influences the PL properties and sensitivity of the

sensors. The ligands can also act as templates, promoting the nucleation and growth of the nanoclusters. In particular, recent advancements have shown that incorporating polymeric or protein-based ligands into the sensor design can lead to enhanced performance, such as increased luminescence and improved dispersibility in aqueous media (Chen et al., 2023; Aires et al., 2018). Additionally, the quantum confinement effects, which arise due to the extremely small size of the metal cores (less than 2 nm), allow MNCs to exhibit unique optical properties, such as size-tunable PL. This tunability is highly desirable for applications in chemical sensing, where precise detection of specific analytes is crucial. For instance, by manipulating the core size or changing the surface ligands, researchers can fine-tune the emission spectra and sensitivity of these sensors for various applications. These combined factors make MNC-based sensors particularly useful for real-time detection of trace analytes in complex environments (Lin et al., 2022; Chen et al., 2019; Xu et al., 2019), opening up further applications in environmental monitoring, biomedical diagnostics and industrial sensing technologies.

The vast advantages offered by functional MNCs in chemical sensing are evident from the significant rise in research publications over the past two decades, underscoring the growing importance of this field (Figure 1). This paper provides a thorough and comprehensive review of MNC-based sensors, with particular emphasis on protein-templated MNCs for chemical sensing applications. The review begins by offering foundational insights into the structural composition and physicochemical properties of
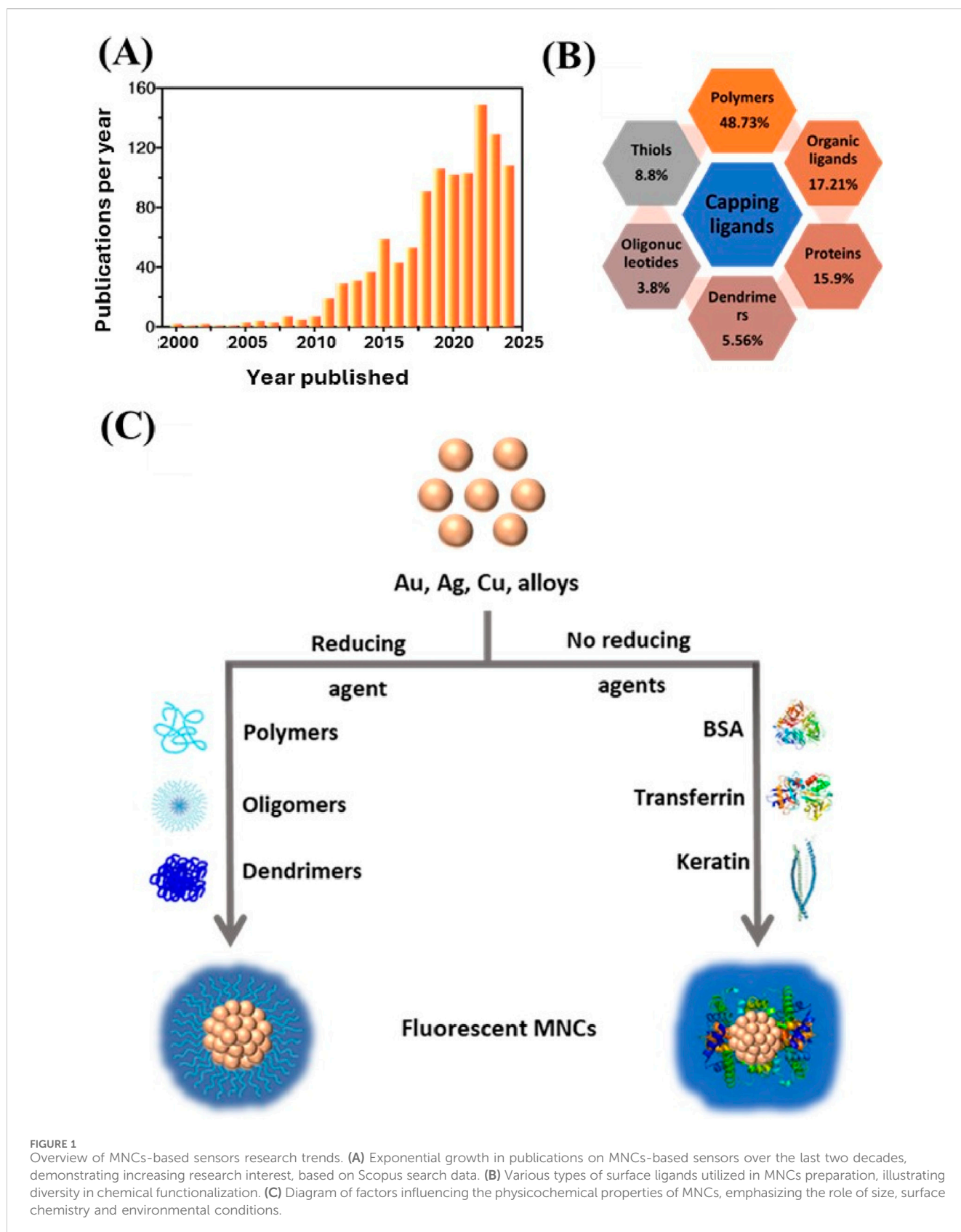
FIGURE 1
Overview of MNCs-based sensors research trends. **(A)** Exponential growth in publications on MNCs-based sensors over the last two decades, demonstrating increasing research interest, based on Scopus search data. **(B)** Various types of surface ligands utilized in MNCs preparation, illustrating diversity in chemical functionalization. **(C)** Diagram of factors influencing the physicochemical properties of MNCs, emphasizing the role of size, surface chemistry and environmental conditions.

MNCs, exploring how these properties influence their function as sensors. Furthermore, it delves into the critical factors affecting the performance of MNC-based sensors, including the impact of metal core size, surface stabilizers and the morphology of the nanoclusters. These factors play a key role in determining the sensitivity, selectivity and efficiency of the sensors. The review also provides

an in-depth comparison of the advantages of using protein templates over polymer and organic ligand templates in the synthesis of MNCs. Protein templates offer superior stability, biocompatibility and functional versatility, making them highly attractive for creating efficient chemical sensors. In addition to reviewing recent advancements in the application of MNCs in chemical sensing, this review offers an extensive analysis of the current literature, providing critical insights into the state of the field. Finally, we discuss the existing challenges and limitations in the development of MNC-based sensors, such as the need for more versatile templates and improved stability under harsh conditions. The review also highlights future research directions, including the potential for expanding the use of MNCs in various sensing applications and the development of more sophisticated synthesis techniques to enhance their performance.

2 Factors effecting the properties of MNCs

The properties of MNCs are significantly influenced by several factors, including the synthesis method, the size and type of metal core, and the nature of the surface ligands. Bottom-up synthesis strategies are widely used for fabricating luminescent MNCs. This approach involves the reduction of metal ions to their zero-valent state in the presence of surface-stabilizing ligands. The resulting nanoclusters possess highly active metal cores with large surface areas, but these bare surfaces can be fragile, making them prone to undesirable side reactions, self-aggregation and structural deformation (Fang et al., 2015). To overcome these challenges, the surface of the metal core must be stabilized through the incorporation of encapsulating agents, which prevent further aggregation and enhance the stability of the nanoclusters.

The physicochemical properties and sensing performance of MNCs, particularly those templated with proteins, are predominantly regulated by the size and type of metal core as well as the surface ligands that protect the core (Tan et al., 2023). The metal core size directly impacts quantum confinement effects, which are responsible for the unique optical and electronic properties of MNCs (Nasrollahpour et al., 2023). Smaller metal cores lead to more pronounced quantum effects, resulting in size-tunable PL, which is a critical feature in chemical sensing applications. The type of metal and alloy also plays a vital role in determining the PL and catalytic activity of the nanoclusters, with Au, Ag, Cu, and Pt being the most commonly used metals due to their favorable optical and chemical properties.

Surface ligands, on the other hand, play a crucial role in stabilizing the metal core and defining the overall characteristics of the MNCs. They form protective layers around the core, preventing its aggregation and modulating the electronic properties by influencing the energy levels involved in PL (Tan et al., 2023). Ligands also offer functionalization possibilities, enabling the MNCs to interact selectively with specific analytes, which is essential for developing highly sensitive and selective chemical sensors. In the case of protein-templated MNCs, the three-dimensional structure of proteins offers numerous functional groups (e.g., amines, thiols, carboxylates) that can bind strongly to metal ions, promoting the nucleation and growth of the

nanoclusters. These proteins not only stabilize the MNCs but also improve their dispersibility in aqueous environments, enhance their biocompatibility and, in some cases, act as reducing agents. This combination of factors contributes to the high stability, tunable PL and excellent sensing capabilities of protein-templated MNCs.

2.1 Metal cores

The properties of the metal core play a fundamental role in determining the PL characteristics of MNCs. The primary source of PL in MNCs is the interband transitions between the occupied d-orbitals and the Fermi level of the metal atoms in the core (Chen P.-C. et al., 2016). These transitions are heavily influenced by the size and type of metal core, which directly impact the optical properties of the nanoclusters. The López-Quintela group demonstrated this through theoretical calculations on copper nanoclusters (Cu NCs), showing that as the size of the copper core increases from Cu_5 to Cu_{20}, the PL peaks shift to longer wavelengths (Vilar-Vidal et al., 2012). This size-dependent shift is attributed to the quantum confinement effect, which becomes more pronounced as the size of the metal core decreases.

The quantum confinement effect is a critical phenomenon in MNCs, where the energy levels are discrete due to the small size of the clusters, leading to tunable PL properties. The Jellium model is often applied to describe the relationship between the number of metal atoms in the clusters and the emission spectra, providing a theoretical framework to calculate the metal core size based on PL measurements (Sinha-Roy et al., 2023; Aikens and Jarrold, 2023). This model explains how the dynamic polarizability of d-electrons affects the dielectric function of the nanocluster due to size-dependent surface imperfections. As a result, the plasmon energy becomes size-dependent, meaning that the reduced d-electron shielding and lower electron density at the metal core's surface layer significantly influence the physicochemical properties of MNCs.

Beyond size, the type of metal used in the core also plays a pivotal role in determining the PL properties of MNCs. Different metals exhibit unique optical and electronic properties, which can be fine-tuned to suit specific applications. Research by Chang's group further highlighted the importance of metal type in PL behavior by studying three distinct types of MNCs: BSA/TSA-Au NCs, BSA/TSA-Ag NCs and BSA/TSA-Cu NCs (Nain et al., 2020). By using an excitation wavelength of 350 nm, they observed distinct PL emission spectra at 700, 624 and 430 nm for Au, Ag and Cu NCs, respectively. These findings underscore the significant impact that both metal type and core size have on the optical characteristics of MNCs.

Moreover, atomically precise MNCs, which have an exact number of metal atoms, offer highly controlled and tunable PL properties (Liu Z. et al., 2024; Xu et al., 2020; Lipok et al., 2023; Li Y. et al., 2021). This precision allows for the fine-tuning of the nanoclusters' light absorption efficiency and emission wavelengths, making them highly versatile for applications such as chemical sensing, bioimaging and catalysis. Atomically precise gold nanoclusters (Au NCs) have shown tunable PL from visible to near-infrared (NIR-I and NIR-II) regions (Liu Z. et al., 2024). By manipulating the size, structure and composition of the Au NCs, researchers have been able to achieve emissions spanning from the

visible spectrum (around 500 nm) to the NIR-II region (up to 1700 nm). This tunability has been facilitated by techniques such as heterometal doping, surface motif rigidification and core phonon engineering, which improve PL quantum yields. When different number of Ag atoms are introduced into the Au_{25} rod, the structure remains intact, but the electronic properties, specifically the HOMO-LUMO energy gap, are altered (Wang et al., 2014). This doping increases the HOMO-LUMO gap, particularly because Ag atoms have higher energy orbitals than Au. The replacement of Au atoms with Ag, starting with the vertex and waist Au atoms, significantly boosts the quantum yield (QY) of PL, with QY values of 8% for pure Au_{25}, 29% for $Ag_{13}Au_{12}$ and 56% for $Ag_{12}Au_{13}$. The enhancement in PL is attributed to the larger energy gap between the ground (S0) and excited (T1) states, which suppresses non-radiative processes and increases radiative efficiency (Mitsui et al., 2022). Despite the small differences in the HOMO-LUMO gap between Au_{25} and Ag-doped clusters, other factors beyond just the energy gap seem to contribute to the significant increase in PL efficiency, warranting further research. Heteroatom doping in Ag and Cu NCs also impacts both radiative and non-radiative processes (Song et al., 2021; Brocha Silalahi et al., 2021; Kang et al., 2016), but more investigation is needed to fully understand the mechanisms behind the improved PL. In summary, the size, type, alloy composition and structural arrangement of the metal core are critical factors that govern the photophysical properties of MNCs. Careful manipulation of these parameters allows for precise control over their optical and electronic behavior. This tunability is key to customizing MNCs for a wide range of applications, including chemical sensing, optical devices and biomedicine.

2.2 Ligands and surface states

Recent studies have moved beyond the traditional quantum confinement view of MNCs, recognizing them as molecular-like entities where surface ligands and states profoundly influence PL properties (Matus and Häkkinen, 2023; Zhang B. et al., 2021; Hossain et al., 2020). Surface ligands, including thiolates, phosphines and biopolymers, not only stabilize the MNCs but also crucially modulate their electronic structures, affecting the energy levels involved in PL processes (Yuan et al., 2020; Häkkinen, 2012; Jin, 2015). The interplay between the metal core and these ligands is pivotal in determining the overall optical behavior of the clusters, where each ligand type brings a distinct influence on stability, optical properties and functional capabilities of MNC sensors.

MNCs typically possess a core-shell structure, featuring an inner metal kernel and outer metal-ligand motifs. These surface metal-ligand motifs are crucial to the PL properties of MNCs, where restricting intramolecular motions has been identified as an effective method to minimize energy loss from photoexcited states via non-radiative relaxation, thus enhancing emission efficiency (Liu Z. et al., 2024). Various methods have been developed to impede these intramolecular motions, thereby inducing rigidity in the surface motifs (Kolay et al., 2022). These include bonding strategies that involve bulky group bonding and other interactions such as hydrogen bonds, dipolar, van der Waals, or electrostatic

interactions, which rigidify the metal-ligand shell, enhancing the PL intensity. For instance, bonding between $Au_{22}(SG)_{18}$ clusters (where, SG = glutathione) and bulky tetraoctylammonium cations has demonstrated significant PL enhancements by making the Au(I)-thiolate shell rigid (Pyo et al., 2015). Furthermore, bis-Schiff base linkages formed between dialdehydes such as 2,6-pyridinedicarboxaldehyde and amino functionalities on $Au_{22}(SG)$ 18 induce cross-linking of Au(I)-SG motifs, leading to significant reductions in non-radiative decay rates and remarkable increase in PL intensity (Pyo et al., 2015).

Other strategies include host–guest interactions, aggregation-induced emission (AIE) and self-locking effects (Guo et al., 2022; Luo et al., 2012). The host–guest self-assembly involves encapsulating smaller molecules within larger host structures, significantly influencing the rigidity of the metal-thiolate shell and promoting radiative decay while suppressing non-radiative processes (Guo et al., 2022). Additionally, the aggregation-induced emission mechanism illustrates how non-luminescent oligomeric Au(I)-thiolate complexes become luminescent upon aggregation (Luo et al., 2012). The self-locking effect utilizes specific surface motifs formed into elongated or interlocked arrangements, reducing non-radiative decay pathways and effectively increasing the quantum yield of radiative decay (Luo et al., 2012). This collective array of strategies highlights a profound and evolving understanding of surface motif rigidification and its pivotal role in enhancing the PL properties of Au NCs.

Traditionally, MNCs have been stabilized by monolayers of small molecules like thiolates and phosphines. However, the shift towards using larger ligands such as polymers, nucleic acids and proteins in the synthesis of MNCs is due to their ability to offer a greater number of functional groups, enabling more versatile and robust interactions with the metal core (van de Looij et al., 2021). This approach not only enhances the stability of the nanoclusters but also allows for the fine-tuning of their optical properties through specific ligand-metal interactions, which is essential for applications that require precise photoluminescent efficiency and specificity. Moreover, larger biomolecules like proteins and nucleic acids introduce biocompatibility, making MNCs particularly suitable for biomedical applications, including drug delivery, bioimaging and biosensing (Zare et al., 2021). The use of polymeric ligands improves the dispersibility of MNCs in various solvents, a crucial attribute for applications in heterogeneous environments where uniform dispersion is necessary. Additionally, the structural diversity and tunable characteristics of these larger ligands permit the design of MNCs with tailored functionalities. These engineered nanoclusters can respond to environmental stimuli or interact specifically with target molecules, thereby broadening their utility across a spectrum of sensing and catalytic applications.

2.2.1 Polymer as template

Polymers have proven to be versatile scaffolding materials for the synthesis and stabilization of MNCs (Qiao et al., 2021; Casteleiro et al., 2021). By varying the polymer templates used in synthesis, researchers can effectively control the size, shape and optical properties of the resulting nanoclusters. This approach has proven effective for a variety of metals, including Au, Ag and Cu, demonstrating the flexibility of polymer-based synthesis. Encapsulation of MNCs within polymers helps prevent

degradation of the nanoclusters during harsh synthesis processes, offering improved stability and functionality in various environments. A wide array of polymers has been employed in this capacity, ranging from naturally derived chitosan to synthetic polyacrylamide, each offering specific benefits depending on the application. *In situ* synthesis during encapsulation often enhances the properties of the nanoclusters, overcoming their inherent instability and offering better protection against aggregation and oxidation during reactions (Casteleiro et al., 2021). Synthetic polymers like poly (methacrylic acid) (PMAA) and poly (vinyl pyrrolidone) (PVP) have shown significant promise in the synthesis of fluorescent MNCs, thanks to their abundant carboxylic and amine groups (Casteleiro et al., 2021). These functional groups interact with metal ions, acting as both a reducing and stabilizing agent. The PL of these nanoclusters can be further tuned by altering polymer properties such as molecular weight, crosslinking density and hydrophobicity.

One of the most exciting applications of polymer-encapsulated nanoclusters is in biomedical fields such as bioimaging and drug delivery. Chitosan, a biodegradable polymer known for its non-toxicity and biocompatibility, has been extensively studied as a vehicle for nanocluster encapsulation (Duan et al., 2018). Its amine groups not only assist in the stabilization of the clusters but also enhance cellular uptake, making chitosan-Au NC composites particularly suitable for *in vivo* applications. Studies have shown that encapsulation within chitosan nanogels significantly increases the PL of Au NCs, allowing for better imaging capabilities under physiological conditions (Wang et al., 2023). In addition to improving imaging, encapsulated Au NCs can be functionalized with various targeting ligands or drugs, making them a powerful tool for theranostics, where diagnostic imaging and therapeutic delivery are combined in a single nanomaterial.

Beyond biomedical applications, encapsulated MNCs have also demonstrated significant utility in catalysis. The interaction between the polymer matrix and the MNCs can modulate the catalytic activity, enhancing reaction specificity and efficiency (Koga et al., 2016). For instance, polystyrene (PS)-encapsulated Au NCs have been shown to be effective catalysts for oxidation reactions, such as the aerobic oxidation of alcohols and boronic acids (Miyamura et al., 2014). The ability of the polymer to control access to the Au NC surface, combined with its inherent chemical stability, makes these nanocomposites promising candidates for industrial-scale catalysis. Furthermore, encapsulation helps prevent aggregation, which is a common issue with unprotected MNCs, ensuring prolonged catalytic activity across multiple reaction cycles.

For chemosensors, Chang's research group has developed several sensors using polymers as template. For example, Lin et al. developed polydiallyldimethylammonium (PDDA)-templated GSH-Au NCs (GSH = glutathione) for the sensing of sulfides (Lin et al., 2021a). Upon excitation at 365 nm, PDDA/GSH-Au NCs exhibited two distinct PL peaks at 620 and 690 nm, corresponding to GSH-Au and PDDA/GSH-Au NCs, respectively. The formation of Au_2S-induced PL quenching in the PDDA/GSH-Au NCs, enabled the detection of sulfide with a linear range of 1–10 μM and a low detection limit of 0.32 μM. Similarly, a polymer-supported Cu NCs using polystyrene sulfonate (PSS) and penicillamine (PA) for hydrogen sulfide detection using a similar method has been reported (Chen P.-C. et al., 2016). By altering the

ratio of PSS during the synthesis, size-tunable PSS-PA-Cu NCs were produced in the range of 173 nm to 5.5 μm. The extent of polymer aggregation on the surface of Cu NCs resulted in the formation of layers that enhanced the dispersibility and stability of the NCs compared to the PA-Cu NCs. The luminescence intensity of as-prepared PSS-PA-Cu NCs becomes higher when increasing PSS ratio to 0.1 wt% and declines with further increasing concentration of PSS. Compared to PA-Cu NCs, smaller-sized PSS-PA-Cu NCs were obtained via metal-thiol interaction with high aqueous dispersibility and luminescence. Hydrodynamic size and zeta potential measurements support the size- and charge-tunability of PSS-PA-Cu NCs in the presence of various modifications of PSS. At 0.05 wt% and 0.1 wt% of PSS concentration, the particle growth is suppressed, resulting in PSS-PA-Cu NCs with a particle diameter of 173 nm. The maximum particle diameter obtained in this report is nearly 5.5 μm in the absence of PSS, indicating that PSS introduction caused size-tunable PSS-PA-Cu NCs. The PL stability of PSS-PA-Cu NCs improved as compared to PA-Cu NCs owing to the ultra-thin coating of PSS on the surface of Cu NCs.

2.2.2 DNA as template

DNA, akin to polymers, functions as an exceptional template for the formation of MNCs, particularly silver nanoclusters (Ag NCs) (Yang et al., 2023). These DNA-templated Ag NCs exhibit unique structural, electronic and photophysical properties, all of which are influenced by the sequence and conformation of the DNA template. This programmable nature of DNA provides an unprecedented ability to fine-tune the properties of nanoclusters by altering parameters such as sequence length, base composition and secondary structures. Consequently, DNA-templated MNCs have found numerous applications in fields like chemical and biomolecular sensing, bioimaging, theranostics and nanophotonics (Xu et al., 2021). The integration of DNA as a template in nanocluster synthesis is driven by its versatility, biocompatibility and molecular programmability, rendering these nanostructures highly promising for advanced technological applications.

The use of DNA as a template for metal nanocluster formation relies on the electrostatic interactions and coordination chemistry between metal ions and the nucleobases of DNA. Each base within a DNA strand offers specific binding sites for metal ions: adenine (A) and cytosine (C) are rich in nitrogen and can form coordination bonds with metal ions, while guanine (G) and thymine (T) offer additional pathways for interaction due to their specific electronic configurations (Song et al., 2019). These interactions facilitate the nucleation and growth of metal nanoclusters along the DNA strand, with the final size, shape and electronic structure of the MNCs being dependent on the sequence and conformation of the DNA template. An excellent example of this phenomenon is the synthesis of silver nanoclusters using polycytosine (poly-C) sequences (O'Neill et al., 2009). Poly-C DNA strands have been shown to preferentially bind silver ions due to their affinity for nitrogenous bases, promoting the formation of highly fluorescent Ag NCs. Furthermore, by varying the length of the poly-C sequence, researchers have been able to precisely control the size of the resulting Ag NCs, with longer sequences producing larger clusters and shorter sequences yielding smaller, more fluorescent nanoclusters (O'Neill et al., 2009). These DNA-templated Ag NCs exhibit excellent stability

in aqueous environments and show a rich variety of fluorescence properties, which can be harnessed for sensing and imaging applications.

One of the most intriguing aspects of DNA-templated nanoclusters is their tunable fluorescence, which can be tailored by modifying the DNA sequence used as a template. This tunability arises because different sequences provide unique spatial arrangements for the nucleation of metal atoms, which in turn affect the electronic structure and energy states of the resulting MNCs (New et al., 2016). For example, Ag NCs templated by guanine-rich DNA sequences often exhibit fluorescence that spans the visible to near-infrared regions (Wen et al., 2020). Moreover, a notable study demonstrated the formation of highly fluorescent DNA-templated Ag NCs using a hairpin DNA structure (O'Neill et al., 2009). The researchers found that altering the base sequences in the stem-loop structure of the hairpin significantly impacted the emission properties of the resulting nanoclusters. Shorter hairpins tended to produce blue-emitting clusters, while longer hairpins favored red or near-infrared emissions. This flexibility allows for the design of highly specific fluorophores that can be used in multiplexed bioimaging or sensing systems, where different emission wavelengths are needed for distinguishing between multiple targets. In addition, specific DNA sequences can induce the self-assembly of nanoclusters into highly organized structures, further enhancing their optical properties. In one example, a Y-shaped DNA scaffold was used to template the formation of Ag NCs that exhibited superior photostability and enhanced fluorescence due to the ordered arrangement of the clusters (Yang et al., 2022). Moreover, by incorporating specific functional groups or sequences into the DNA template, researchers can fine-tune the interaction between the metal atoms and the DNA, resulting in clusters with tailored properties. For example, thiolated DNA (DNA-SH) has been used to template Ag NCs, where the sulfur-containing thiol groups provide additional binding sites for silver ions, stabilizing the nanocluster and enhancing its fluorescence (Zhang et al., 2018). This approach has been particularly effective in preventing the oxidation of Ag NCs, which is a common issue in the synthesis of silver-based nanostructures.

Moreover, the versatility of DNA templates extends beyond Ag to other metals, including Au and Cu, which further expands the potential applications of DNA-templated MNCs (Wang et al., 2019; Li P. et al., 2023; Zhang et al., 2019). Au NCs, for instance, have been synthesized using DNA templates and have exhibited tunable fluorescence similar to Ag NCs (Wang et al., 2019). These Au NCs, due to their excellent photostability and biocompatibility, are particularly well-suited for bioimaging applications. DNA-templated Au NCs could be used for cellular imaging, where their NIR emission enabled deep tissue penetration, making them highly effective for non-invasive imaging techniques. The potential of DNA-templated MNCs extends beyond Ag NCs and Au NCs to bimetallic clusters, which combine the properties of two different metals to create nanostructures with enhanced functionality (Zaleska-Medynska et al., 2016). Bimetallic clusters, such as Au-Ag or Au-Cu, have been templated using DNA to create nanoclusters with unique optical and catalytic properties (Sun et al., 2019; Pei et al., 2024). For instance, DNA-templated Au-Ag nanoclusters have been shown to exhibit enhanced catalytic

activity for the reduction of 4-nitrophenol, a model reaction commonly used to test the catalytic efficiency of metal nanoparticles (Zhou et al., 2019).
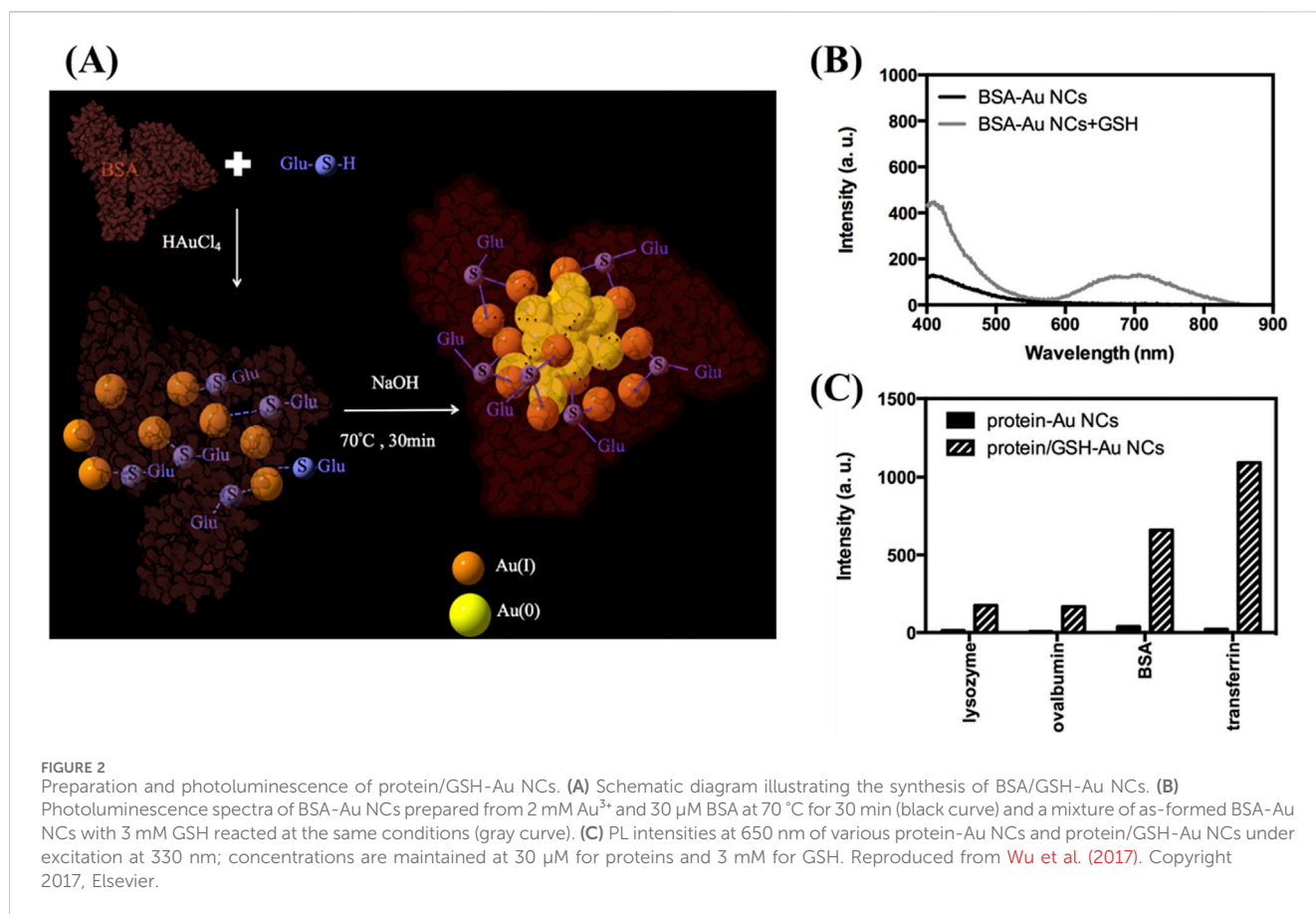
DNA-templated MNCs have shown remarkable potential in the development of chemical and biomolecular sensors, owing to their tunable fluorescence, high sensitivity and selective binding capabilities. These properties are particularly advantageous in biosensing, where the detection of specific analytes such as metal ions, nucleic acids and proteins is of paramount importance (Song et al., 2019; Tang et al., 2024; Yang et al., 2023). For instance, DNA-templated Ag NCs have been successfully employed as highly sensitive probes for the detection of metal ions, such as mercury (Hg^{2+}) and copper (Cu^{2+}) (Song et al., 2019; Li and Wei, 2017). In a typical sensing mechanism, the presence of the target metal ion induces a conformational change in the DNA template, which in turn alters the fluorescence of the bound nanocluster (Chen Y.-C et al., 2016). For example, a study demonstrated the use of DNA-templated Ag NCs to detect Hg^{2+} ions in water samples with a detection limit as low as parts-per-billion (ppb). The binding of Hg^{2+} to thymine-rich regions of the DNA scaffold led to quenching of the fluorescence signal, enabling highly sensitive and selective detection (Guo et al., 2021).

2.2.3 Protein as template

Protein-templated metal nanoclusters (MNCs) have emerged as ideal candidates for various nanotechnology applications due to their bioavailability, biocompatibility, ease of functionalization and ability to form stable, water-soluble complexes (Guo et al., 2021; López-Domene et al., 2023; Lettieri et al., 2021; Suo et al., 2019). These advantages, coupled with the unique properties conferred by proteins, have positioned protein-templated MNCs as highly attractive for use in chemical sensing, bioimaging, catalysis and theranostics (Duan et al., 2018). Unlike other surface capping agents, such as synthetic polymers or small molecules, the inherent three-dimensional structure of proteins offers an abundance of functional groups (e.g., amines, thiols, carboxylates) that facilitate the binding of metal ions and promote the nucleation and growth of MNCs (Zare et al., 2021; Chakraborty and Parak, 2019; Yu et al., 2020; Cheng et al., 2023). This enables precise control over the size, structure and photophysical properties of the resulting nanoclusters.

The ability of proteins to act as templates for MNC formation is due to their intricate folded structures, which provide binding sites that stabilize the metal cores and prevent undesirable aggregation (Qiao et al., 2021; Kailasa et al., 2021). For example, bovine serum albumin (BSA), a commonly used protein template, has been shown to stabilize Au NCs through strong interaction between its cysteine residues and the gold atoms (Xie et al., 2009). This results in Au NCs with enhanced PL properties, which are critical for applications in bioimaging. Research has shown that protein-templated Au NCs can exhibit size-tunable fluorescence, with emission wavelengths ranging from the visible to the near-infrared region, depending on the specific protein used and its interaction with the gold atoms (Tan et al., 2023).

The PL of protein-templated MNCs is largely determined by the interaction between the metal atoms and the protein's functional groups (Qiao et al., 2022; Voet and Tame, 2017; Czyżowska et al., 2021; Yarramala et al., 2017). The sulfur-containing thiol groups of cysteine residues, in particular, play a crucial role in the formation of

FIGURE 2
Preparation and photoluminescence of protein/GSH-Au NCs. **(A)** Schematic diagram illustrating the synthesis of BSA/GSH-Au NCs. **(B)** Photoluminescence spectra of BSA-Au NCs prepared from 2 mM Au³⁺ and 30 μM BSA at 70 °C for 30 min (black curve) and a mixture of as-formed BSA-Au NCs with 3 mM GSH reacted at the same conditions (gray curve). **(C)** PL intensities at 650 nm of various protein-Au NCs and protein/GSH-Au NCs under excitation at 330 nm; concentrations are maintained at 30 μM for proteins and 3 mM for GSH. Reproduced from Wu et al. (2017). Copyright 2017, Elsevier.

Au-S bonds, which contribute to the stability and PL properties of the nanoclusters. For instance, studies by Chang's group demonstrated that the cysteine content of the protein template can significantly influence the PL intensity of Au NCs (Wu et al., 2017). By manipulating the cysteine content or adding exogenous thiol compounds such as glutathione (GSH), it is possible to reduce the amount of protein required for nanocluster synthesis while still maintaining high PL yields (Figure 2).
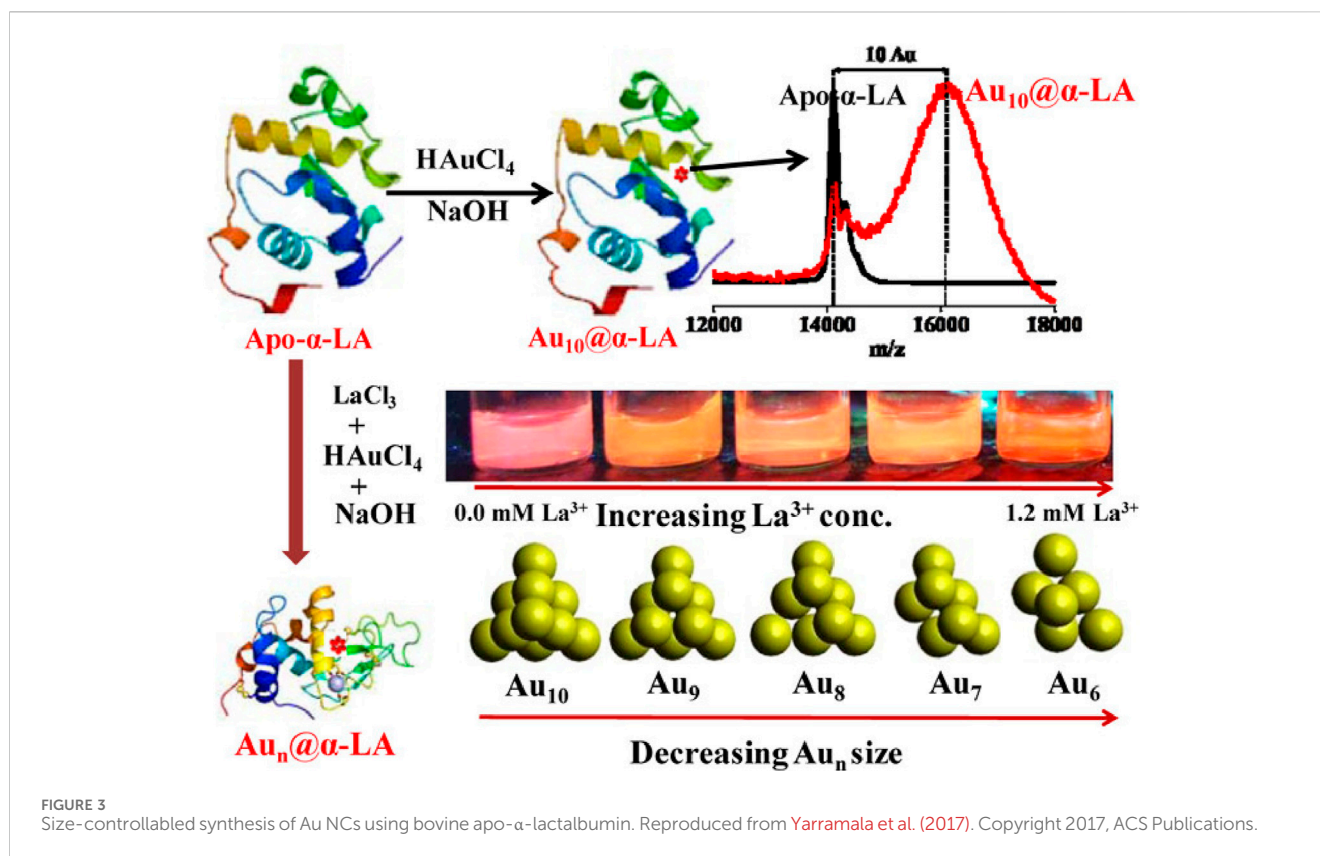
The influence of cysteine residues on the formation of protein-based Au NCs was further validated by Chen's group through detailed mass spectrometry analysis (Hsu et al., 2019). Their investigation revealed that gold atoms preferentially bind to cysteine sites and selectively attach to disulfide groups within the protein structure. The primary capping sites for red-emitting Au NCs were identified as C75–C91/C90–C101 in domain IA, C315–C360/C359–C368 in domain IIB and C513–C558/C557–C566 in domain IIIB. Peptides containing oxidized cysteines, such as sulfinic or cysteic acids, were found to be the main reducing agents, predominantly located outside the core regions of the protein. This observation suggests that the oxidation-induced cleavage of disulfide bonds, coupled with accompanying conformational changes in the protein facilitated the subsequent nucleation and growth of nanoclusters near intact disulfide pairs.

The versatility of protein templates extends to their ability to form nanoclusters with metals other than Au, such as Ag and Cu. For instance, Ag NCs templated by BSA have been shown to exhibit strong PL and excellent colloidal stability, making them suitable for use in sensing and bioimaging applications (Sarkar et al., 2023). Similarly, Cu NCs have been templated using proteins such as lysozyme and hemoglobin (Sebastian et al., 2023), which provide a biocompatible scaffold that enhances the stability and functionality of the Cu NCs in aqueous environments.

A key advantage of using proteins as templates for MNC synthesis is their ability to act as reducing agents in addition to providing structural stability. This dual functionality simplifies the synthesis process by eliminating the need for external reducing agents, which are typically required in other MNC synthesis methods. For example, Yarramala et al. successfully synthesized size-controllable Au NCs using bovine apo-α-lactalbumin (apo-α-LA), a protein with specific binding sites for calcium and lanthanum ions (Yarramala et al., 2017). Apo-α-LA interacts with Au³⁺ ions, facilitating both the formation of Au₁₀ clusters and the reduction of Au³⁺ to the Au⁰ state. The protein effectively inhibits excessive particle growth, yielding Au NCs of varying sizes, including Au₁₀, Au₉, Au₈, Au₇ and Au₆. The presence of apo-α-LA significantly enhances the surface stability and luminescence properties of the Au NCs, making the protein a crucial factor in maintaining their structural and optical integrity (Figure 3).

Other studies have explored the use of different proteins as templates for MNC synthesis, each offering unique advantages based on their size, amino acid composition and structural properties. Bao's group, for instance, demonstrated that the size of the protein template and its amino acid content, particularly the balance of

FIGURE 3
Size-controllabled synthesis of Au NCs using bovine apo-α-lactalbumin. Reproduced from Yarramala et al. (2017). Copyright 2017, ACS Publications.

amine and tyrosine/tryptophan residues, play a crucial role in the formation and stabilization of Au NCs (Xu et al., 2014). Their study revealed that smaller proteins with fewer cysteine residues tend to produce Au NCs with a blue shift in fluorescence emission and shorter fluorescent lifetimes. This suggests that amino acids other than cysteine, such as tryptophan, may also contribute to the stabilization and optical properties of the nanoclusters.

In addition to the well-documented use of BSA, other proteins such as chicken egg white (CEW) protein and hemoglobin have been successfully employed as templates for MNC synthesis (Zare et al., 2021; Akyüz et al., 2020; Cun et al., 2023). Apak's group, for example, synthesized Au NCs with high PL properties using CEW protein as both a protecting and reducing agent. The resulting Au NCs exhibited a broad emission peak at 640 nm, with excellent stability and biocompatibility, making them ideal candidates for biosensing and imaging applications (Akyüz et al., 2020).

In summary, protein-templated MNCs represent a versatile and highly effective platform for the synthesis of stable, biocompatible and functional nanoclusters. The unique properties of proteins, including their abundance of functional groups and ability to act as both stabilizers and reducing agents, make them ideal candidates for templating MNCs. The tunable optical properties, excellent colloidal stability and biocompatibility of protein-templated MNCs have enabled their widespread use in applications such as sensing, bioimaging, catalysis and theranostics. As research continues to explore new protein templates and synthesis strategies, the potential of protein-templated MNCs is likel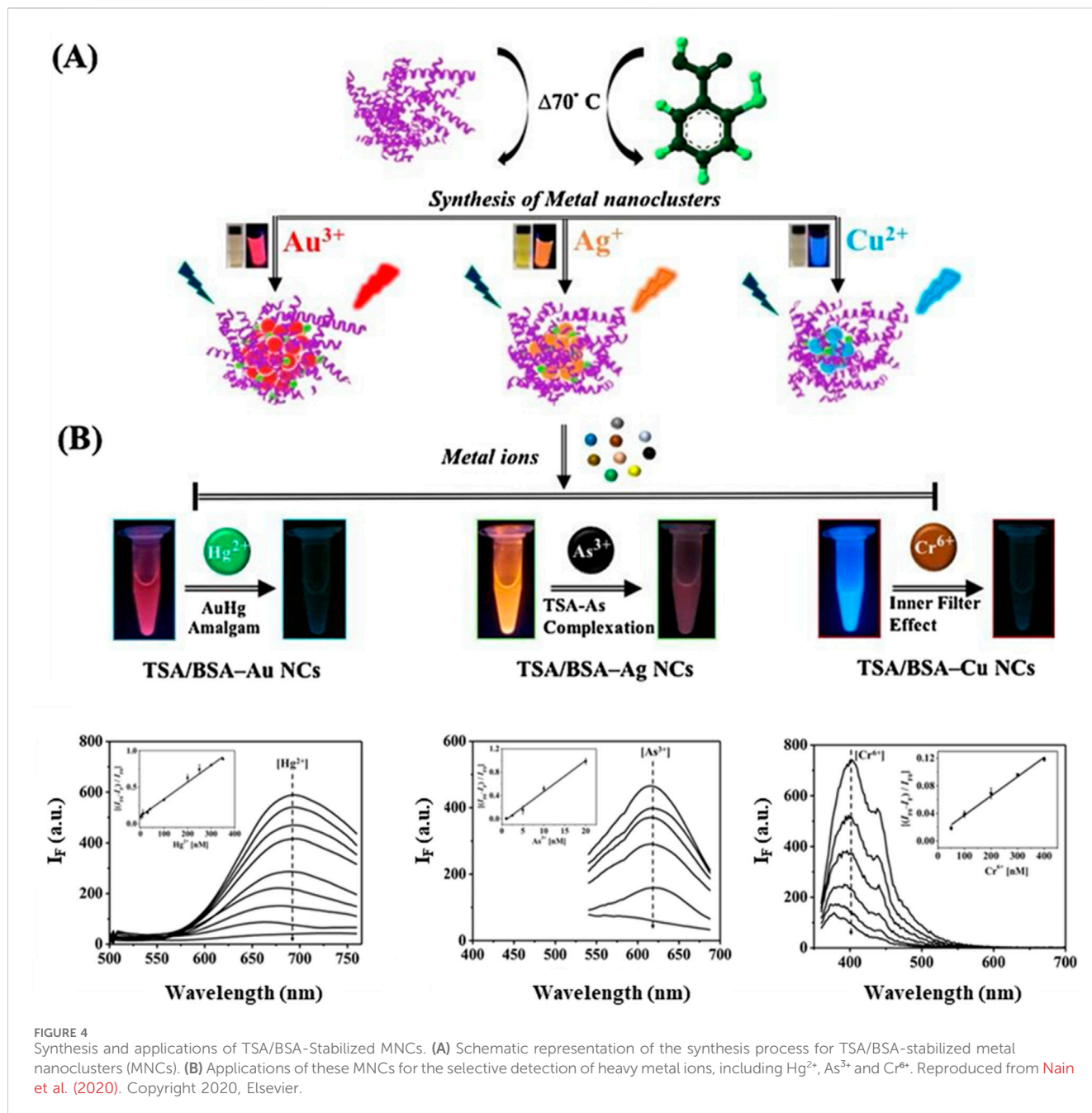y to expand further, offering exciting opportunities for the development of advanced nanomaterials for a wide range of scientific and technological applications.

3 Protein-templated MNCs as PL probe

3.1 On-off sensors

In signal-off biosensing strategies involving protein-templated MNCs, the PL of the NCs is quenched in the presence of specific analytes. This quenching effect can occur via two primary mechanisms (Panthi and Park, 2022; Tan et al., 2023). First, the analyte may interact directly with the protein, disrupting its protective function and exposing the metal core. In the second mechanism, the analyte binds to the metal core itself, causing structural changes that reduce the PL intensity. In both cases, the reduction in PL is proportional to the concentration of the analyte, forming the basis for signal-off biosensing.

The protein structure plays a critical role in this process due to its numerous functional groups, such as carboxyl, amine and sulfhydryl groups, which are readily available to bind quenching agents. Metal ions are the most commonly used quenchers, given their strong affinity for the functional groups on the protein surface. Proteins such as BSA, lysozyme and hemoglobin are frequently used as templates because they provide a robust scaffold for the formation of MNCs and offer a rich array of functional groups that can bind analytes. For instance, lysozyme-templated Ag NCs have been employed to detect glutathione, where the binding of glutathione leads to a reduction in fluorescence (Sam et al., 2024). This

FIGURE 4
Synthesis and applications of TSA/BSA-Stabilized MNCs. **(A)** Schematic representation of the synthesis process for TSA/BSA-stabilized metal nanoclusters (MNCs). **(B)** Applications of these MNCs for the selective detection of heavy metal ions, including Hg^{2+}, As^{3+} and Cr^{6+}. Reproduced from Nain et al. (2020). Copyright 2020, Elsevier.

interaction between the analyte and the protein-templated MNCs is highly specific, enabling selective detection of target analytes in complex biological samples. For example, BSA-templated Au NCs have been shown to exhibit significant quenching in the presence of Hg^{2+} ions, which bind to cysteine residues and disrupt the Au-S bonds that stabilize the nanoclusters (Chen et al., 2013). This results in a loss of fluorescence, allowing for highly sensitive detection of mercury. Furthermore, Nain et al. has synthesized various Au, Ag and Cu NCs protected by BSA and thiosalicylic acid (TSA), each exhibiting PL emissions at wavelengths of 700, 624 and 430 nm, respectively (Nain et al., 2020). These NCs enable the sensitive detection of Hg^{2+}, arsenic (As^{3+}) and Cr^{6+} ions by utilizing PL quenching, achieving a low detection limit in the nanomolar range (Figure 4).

In addition to their use in detecting metal ions, protein-templated MNCs have been applied to the detection of small molecules and biomolecules. For example, BSA-templated Au NCs have been used to detect GSH (Wong et al., 2021), a key antioxidant in biological systems. The interaction between GSH and the metal core of the Au NCs disrupts the PL emission, providing a simple and effective method for GSH quantification. In another study, Chang's group presents a dual-emission BSA-Au NC probe for the detection and quantification of cathinone analogues, in aqueous solutions. Upon interaction with cathinone drugs, the PL of the BSA-Au NCs in the 650 nm range was quenched while the 460 nm PL remained unaffected causing a color shift from red to dark blue, allowing for detection limits as low as 0.14 mM and a PL color-change threshold of 10.0 mM for 4-chloromethcathinone

(Yen et al., 2019). These examples highlight the versatility of protein-templated MNCs in signal-off biosensing, offering a wide range of applications from environmental monitoring to biomedical diagnostics.

In summary, the signal-off biosensing strategy utilizing protein-templated MNCs relies on the interaction between the analyte and the metal core or protein scaffold, leading to a measurable reduction in PL. The abundance of functional groups on protein templates makes them ideal for binding quenching agents, particularly metal ions and the inherent stability and biocompatibility of proteins enhance the performance of these biosensors. As research into protein-templated MNCs continues to advance, new opportunities for improving sensitivity, selectivity and application diversity will emerge, solidifying their role in biosensing technologies for environmental and biomedical applications.

3.2 Off-on sensors

Off-on sensors represent a sophisticated and versatile approach in the design of biosensors based on MNCs. In this strategy, the PL of the MNCs is initially quenched through interaction with a quenching mediator. The introduction of the target analyte subsequently triggers a competitive interaction, where the quenching mediator binds preferentially to the analyte rather than the MNCs (Duan et al., 2018; Zhu et al., 2019; Dong et al., 2021). This competitive binding results in the restoration of the PL signal, which had initially been suppressed. This off-on approach has become a highly valuable tool in biosensing due to its sensitivity and the ease with which PL changes can be monitored, offering significant promise for detecting biomolecules, metal ions and other relevant analytes.

In a typical off-on sensor, the initial quenching phase is achieved by introducing a quenching mediator, such as metal ions or other small molecules, that interacts with the metal core or functional groups on the MNCs. For example, BSA-Au NCs have been used extensively in such sensors, where quenching agents such as Fe^{3+} or Cu^{2+} ions are employed (Duan et al., 2018; Zhu et al., 2019). These metal ions bind to the sulfur atoms of the BSA-Au NCs, forming non-radiative complexes that effectively dampen the PL. Once the target analyte is introduced, it displaces the quenching agent, restoring the PL. The restoration of the fluorescence serves as a signal that the analyte has successfully been detected. This mechanism provides a clear and direct means of detecting the presence of specific targets, making it highly effective for applications in biomedical diagnostics and environmental monitoring.

One of the key advantages of the off-on strategy is its ability to achieve highly sensitive detection limits. For instance, Ding et al. demonstrated an innovative approach using BSA-Au NCs coated on nanopipettes for the detection of bio-thiols such as cysteine (Ding et al., 2020). The nanopipettes provide a confined space that enhances the interaction between the target analyte and the nanoclusters. In this system, the PL of the BSA-Au NCs is initially quenched, but the presence of cysteine reverses the quenching, restoring the fluorescence. This method achieved a remarkable detection limit of 1 fM (fM) and a dynamic range of 0.001–1 pM (pM), highlighting the sensitivity of the system. The

combination of electrochemical and fluorometric detection in this method further enhanced its versatility, allowing for more precise monitoring of analytes in complex biological environments.

Another compelling example of the off-on strategy is found in the work of Deng et al., who developed BSA/3-mercaptopropionic acid (MPA) co-modified Au NCs for the detection of pyrophosphate (PPi) (Deng et al., 2020). In this system, Fe^{3+} ions act as quenching mediators, suppressing the PL of the BSA-MPA Au NCs. The introduction of PPi results in the chelation of Fe^{3+} ions, effectively removing them from the MNCs and restoring the PL signal. This off-on sensor was further employed to detect alkaline phosphatase (ALP) activity in human osteosarcoma cells. The competitive interaction between Fe^{3+} ions and PPi allowed for a highly sensitive detection of ALP, with a linear detection range of 0.8–16 UL^{-1} and a detection limit of 0.78 UL^{-1}. This system demonstrates the potential of off-on sensors to be used in real-world biological applications, where detecting enzyme activity in cells can be crucial for diagnosing and monitoring diseases.

In summary, off-on sensors based on MNCs represent a highly versatile and sensitive approach for detecting a wide range of analytes, from metal ions to small biomolecules. The use of a quenching mediator that can be displaced by the target analyte allows for the restoration of the PL signal, providing a clear and measurable readout. The adaptability of this approach, combined with its ability to integrate multiple detection modalities and perform multiplexed detection, makes off-on sensors a powerful tool for biosensing and diagnostics. As research continues to refine the design of MNCs and quenching mediators, off-on sensors are likely to play an increasingly important role in fields such as environmental monitoring, medical diagnostics and point-of-care testing.

3.3 Ratiometric sensors

Ratiometric detection is a more advanced and reliable technique compared to traditional single-wavelength methods, particularly in the field of sensing using MNCs. In ratiometric detection, PL intensities at two distinct wavelengths are measured and the ratio of these intensities is used as the primary readout. This ratio provides an internal reference that helps mitigate potential environmental variations, such as fluctuations in light intensity, probe concentration, or surrounding conditions, which can otherwise affect the accuracy of single-wavelength measurements. This approach is particularly advantageous in enhancing the sensitivity and accuracy of the probe for quantification purposes. By comparing the PL intensities at two wavelengths, it becomes easier to detect even small changes in analyte concentration with higher precision.

Ratiometric detection has been successfully applied in various MNC-based sensing platforms. For instance, in the detection of heavy metal ions like Hg^{2+}, ratiometric sensors utilizing Au and Ag NCs can measure the intensity changes at two wavelengths corresponding to the nanoclusters' emission and the analyte-induced spectral shift (Li et al., 2019). This dual-wavelength comparison enhances the accuracy of detecting small concentrations of Hg^{2+}, even in complex biological or environmental samples, where matrix effects might otherwise interfere with single-wavelength readings.
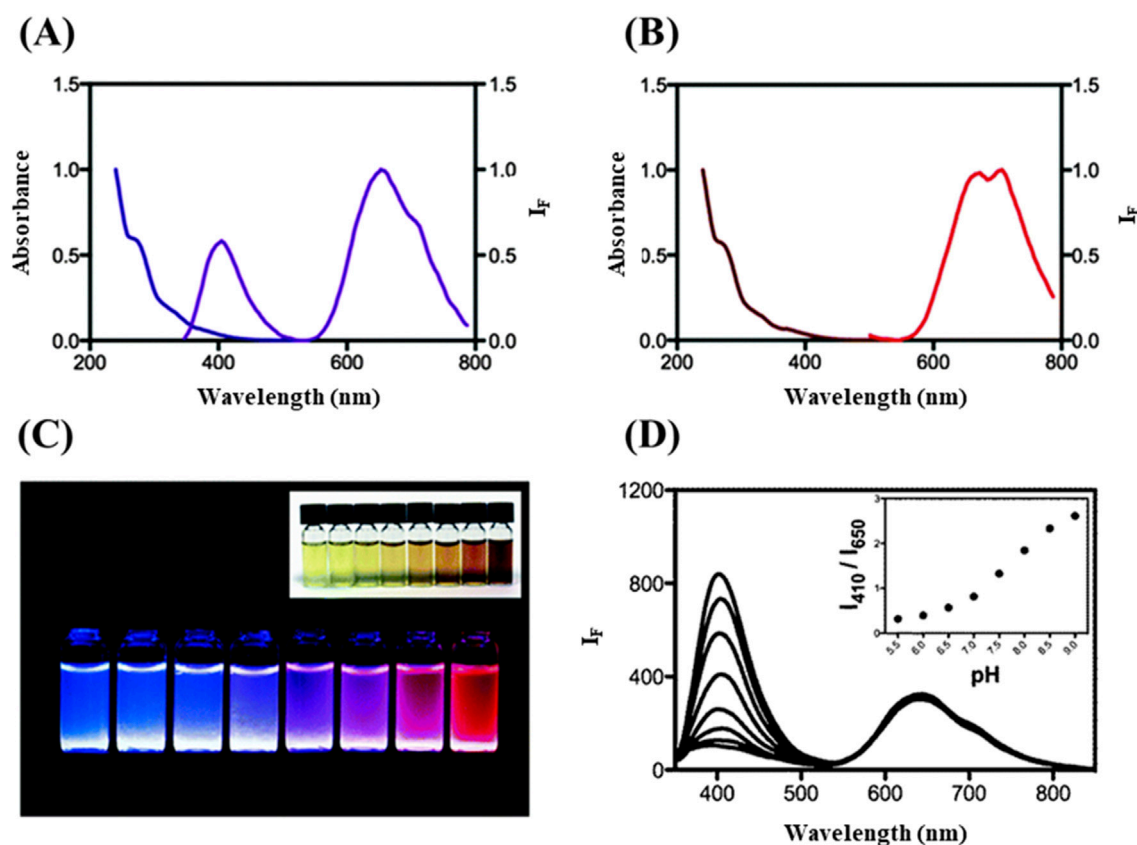
FIGURE 5
Spectroscopic analysis of BSA-Ce/Au NCs and its application for pH monitoring. **(A)** Absorption and PL spectra of BSA−Ce/Au nanoclusters. **(B)** Spectra for BSA-Au nanoclusters. **(C)** Photographic representation of photoluminescent solutions of BSA with Ce(IV) and Au(III) across different molar ratios; BSA concentration is maintained at 0.76 mM, with Ce(IV)/Au(III) ratios ranging from 1,000/0 to 0/10. **(D)** PL responses of BSA−Ce/Au NCs in 20 mM phosphate buffer across pH values from 5.5 to 9.0, with inset showing PL intensity ratios at 410 and 650 nm across these pH values. Reproduced from Chen et al. (2014). Copyright 2014, Royal Society of Chemistry.

The introduction of additional metal ions can be used to provide additional fluorophores that provide PL at different wavelengths. For example, Chang's group developed a one-pot synthesis of photoluminescent BSA-stabilized Ce/Au NCs, which were used as ratiometric pH probes (Figure 5) (Chen et al., 2014). These nanoclusters exhibited dual-emission properties, with distinct PL intensities at two wavelengths that varied depending on the pH of the solution. One emission at ca. 650 nm remained relatively constant, serving as an internal reference, while another emission intensity at ca. 410 nm shifted in response to changes in pH. This ratiometric approach allowed for precise and accurate measurement of pH levels across a wide range, making the BSA−Ce/Au nanoclusters highly effective for biological and environmental sensing applications. The internal referencing provided by the ratiometric system enhanced the reliability of pH measurements compared to traditional single-wavelength methods, where environmental fluctuations could lead to inaccurate readings. BSA−Ce/Au NCs can also be used for the detection of cyanide ions (CN^-). As the concentration of CN^- increased, the PL intensity of the BSA−Ce/Au NCs at 658 nm gradually decreased due to the dissolution of the Au NCs, while the intensity at 410 nm increased. This dual response enabled the detection of CN^- with a detection limit as low as 50 nM and a linear detection range from 0.1 to 15 μM

(Wang C W et al., 2016). Similarly, Li et al. incorporated Eu^{3+} ions into BSA-Au NCs and applied for the detection of dipicolinic acid (DPA) with a low detection limit of 0.8 μM (Li X. et al., 2021). This was also applied in the detection of DPA released during the germination of *Bacillus subtilis* spores.

Xiao et al. developed two types of PL emitting BSA-Au NCs by synthesizing them at different pH levels, which allowed for distinct emission profiles (Xiao et al., 2020). These two types of Au NCs were subsequently combined into a single thin film using a layer-by-layer (LBL) assembly technique. The resulting thin film exhibited dual PL peaks when excited at 372 nm, corresponding to blue emission at 443 nm and red emission at 622 nm from the two Au NC types, respectively. This ratiometric system enabled highly sensitive detection of bilirubin, where the interaction of bilirubin with the Au NCs caused differential quenching of the two emission peaks. This differential quenching allowed for ratiometric detection of bilirubin with a limit of detection (LOD) of 8.90 nM in serum samples, demonstrating the effectiveness of ratiometric sensing for biological applications.

Similarly, Wu et al. utilized BSA-Au NCs in combination with BSPOTPE, an AIE active molecule, as detection and reference probes, respectively, for glucose sensing in a GOx detection system (Wu et al., 2020) (Figure 6). In this system, the H_2O_2
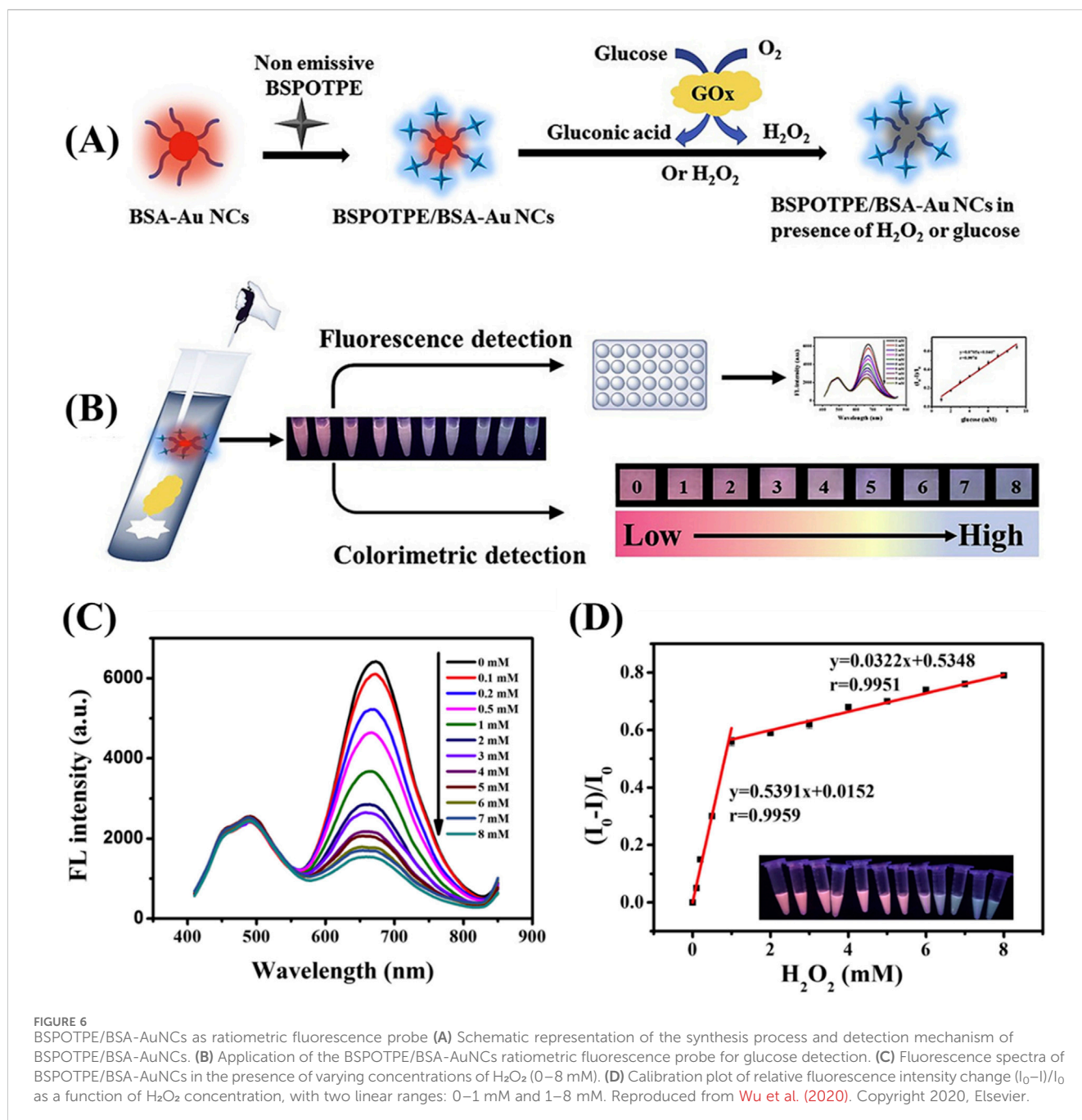
FIGURE 6
BSPOTPE/BSA-AuNCs as ratiometric fluorescence probe **(A)** Schematic representation of the synthesis process and detection mechanism of BSPOTPE/BSA-AuNCs. **(B)** Application of the BSPOTPE/BSA-AuNCs ratiometric fluorescence probe for glucose detection. **(C)** Fluorescence spectra of BSPOTPE/BSA-AuNCs in the presence of varying concentrations of H_2O_2 (0−8 mM). **(D)** Calibration plot of relative fluorescence intensity change $(I_0−I)/I_0$ as a function of H_2O_2 concentration, with two linear ranges: 0−1 mM and 1−8 mM. Reproduced from Wu et al. (2020). Copyright 2020, Elsevier.

produced by the enzymatic reaction of glucose with GOx induced the oxidation of the Au NCs, resulting in a decrease in their PL intensity. However, BSPOTPE, which remains photoluminescent, served as a stable reference probe, allowing for accurate ratiometric detection of glucose. This system achieved glucose detection down to 1 mM under UV light, demonstrating the potential of combining BSA-Au NCs with AIE-active molecules for sensitive and reliable biosensing.

The ratiometric sensors are particularly advantageous in complex biological and environmental samples, where fluctuations in external factors such as light intensity, probe concentration and environmental conditions can otherwise compromise the accuracy of single-wavelength measurements. By using ratiometric sensing, these variations are effectively minimized, leading to more precise and reproducible results. Furthermore, the ability to integrate ratiometric detection into multiplexed sensor systems enhances their utility for simultaneous detection of multiple targets, further expanding their applicability in point-of-care testing and real-time monitoring. Looking forward, the continued refinement of nanomaterials and the development of innovative ratiometric sensor designs, such as dual-emission nanoclusters and integration with AIE molecules, offer exciting opportunities for even greater sensitivity, selectivity and functional flexibility. As the field progresses, ratiometric sensors are poised to play an increasingly vital role in precision diagnostics, environmental sensing and a wide array of applications where robust and reliable detection is essential.

3.4 MNCs-based composite sensors

Recent efforts have been made to enhance the PL sensing capabilities of MNCs by incorporating non-metallic elements into their structure. These non-metallic elements, such as carbon, nitrogen, phosphorus and sulfur offer unique electronic and chemical properties that can improve the PL efficiency and sensing performance of MNCs. These attempts to integrate non-metallic elements not only improve the optical performance of MNCs but also open new avenues for developing multifunctional sensors with superior selectivity and responsiveness. Materials such as metal-organic framework (MOF), carbon nanomaterials and porous silica have been introduced into the MNCs to form a new kind of sensing probe. For instance, Khataee et al. reported dual emissive PL probe fabricated by encapsulating both Au NCs and Cu NCs into zeolitic imidazolate framework-8 (ZIF-8) and the obtained composite (AuCu NCs@MOF) was utilized for ratiometric determination of tetracycline (Tcy) antibiotic (Khataee et al., 2020). The logarithm of the PL ratio against the concentration of Tcy exhibited a linear range from 20 to 650 nM with a detection limit of 4.8 nM. The probe was applied for Tcy quantification in milk samples with superior results. Kong et al. designed a novel dual-emission reverse change ratio PL nanoplatform for fluorimetric and colorimetric sensing of heparin (Hep) and chondroitin sulfate (CS) based on green emissive terbium metal-organic framework (Tb MOF) and red emissive BSA@Au NCs (Kong et al., 2022).

In collaboration with Chang's research group, Chen's team developed a handheld pathogen sensor using a paper-based analytical device (µPAD) for rapid and sensitive pathogen detection (Yuan et al., 2022). This detection system utilizes graphene quantum dots (GQDs) and Au NCs, which are conjugated with antibodies to produce a colorimetric signal in the presence of pathogenic antigens. The sensor exhibited excellent performance, with linear detection ranges for protein A and exotoxin A between 0.3 and 30 ng/mL and detection limits of 0.2 ng/mL and 0.1 ng/mL, respectively. Additionally, Hu et al. designed a ratiometric detection system employing Au NCs as the probe and vesicle carbon dots (VCDs) as the internal standard (Figure 7) (Hu et al., 2022). This configuration confines Au NCs, enzymes and analytes within VCDs to increase local concentrations and improve assay sensitivity. In this study, cholesterol oxidase (ChOX) was used as a model enzyme for cholesterol quantification. The H_2O_2 produced through the enzymatic reaction caused PL quenching of the Au NCs (emission at 670 nm), while the VCDs (emission at 400 nm) remained unaffected. This ratiometric PL method enabled the detection of H_2O_2 within a range of 1–100 µM, with a detection limit of 0.673 µM and cholesterol concentrations ranging from 5 to 100 µM, with a detection limit of 2.8 µM, making it suitable for evaluating cholesterol levels in human serum samples.

The nanocomposite (BCD@SiO$_2$@Au NCs) served as a ratiometric photoluminescent sensor for the selective detection of Gram-negative bacteria, exploiting the copper-homeostasis mechanism inherent to these bacteria (Figure 8). The sensor's principle of detection relies on the quenching effect of Cu^{2+} on Au NCs and the concurrent reduction of Cu^{2+} by Gram-negative bacteria, demonstrating strong selectivity (Fu et al., 2022). In a related research by Zhang et al., a ratiometric photoluminescent

probe (CQDs-Au NCs) was developed by combining amidated carbon quantum dots (CQDs) with BSA-coated Au NCs. This probe displayed dual emission peaks at 446 nm and 670 nm, producing purple PL upon excitation at 397 nm. The probe's effectiveness is attributed to the quenching of this purple PL by dopamine (DA), which occurs via electron transfer from the CQDs to DA, inhibiting the Förster resonance energy transfer (FRET) between CQDs and Au NCs. This ratiometric probe selectively detects DA, with a detection limit of 2.66 nM and a linear response spanning several concentration ranges: 2.66 nM–0.18 mM, 0.511–3.79 mM and 4.87–13.1 mM (Zhang Y et al., 2021).

Looking forward, future directions for MNC-based composite sensors will likely focus on the continued development of hybrid systems that leverage the unique properties of both MNCs and functional materials. One promising area is the exploration of novel MOFs and carbon-based nanomaterials that can further enhance the stability and PL efficiency of MNCs, particularly in challenging environments such as highly acidic or oxidative conditions. Additionally, the incorporation of responsive materials, such as stimuli-sensitive polymers or smart hydrogels, could lead to the creation of dynamic sensing platforms capable of adapting to real-time changes in their environment.

4 Summary and prospects

MNCs have seen significant advancements over the past decades and have become integral to various *in vitro* and *in vivo* detection applications. Protein-templated MNCs have facilitated the synthesis of nanoclusters with precise atomic numbers, ultra-small sizes and low toxicity, enabling their use in a wide range of sensing platforms. These include the detection of small molecules, metal ions and biological species, as well as *in vivo* imaging. One of the most promising developments in this field is the rise of MNC-based ratiometric sensing, which provides greater accuracy compared to traditional on-off or off-on sensing mechanisms. Additionally, the integration of composite materials into MNC platforms has further enhanced the sensitivity and accuracy of these sensors, making them more effective for real-world applications.

Despite these advancements, several challenges and limitations still exist in the development of MNCs, particularly in their broader adoption in environmental, clinical and industrial settings. One of the primary challenges is the limited variety of protein templates available for MNC synthesis. While proteins such as BSA have been widely used, the diversity of templates is still lacking, limiting the potential to create MNCs with tailored properties. Moreover, the use of functional proteins like antibodies or enzymes as templates is not well-established, partly because their biological activity is often compromised during synthesis. This functional loss, coupled with the high cost of functional proteins, remains a significant barrier to their widespread application. Though the use of GSH has been shown to reduce the required concentration of protein for cluster formation, the cost of biologically significant proteins is still prohibitive for large-scale use.

Another limitation is the narrow range of metal cores used in MNCs, with most research focusing on Au, Ag and Cu. While other
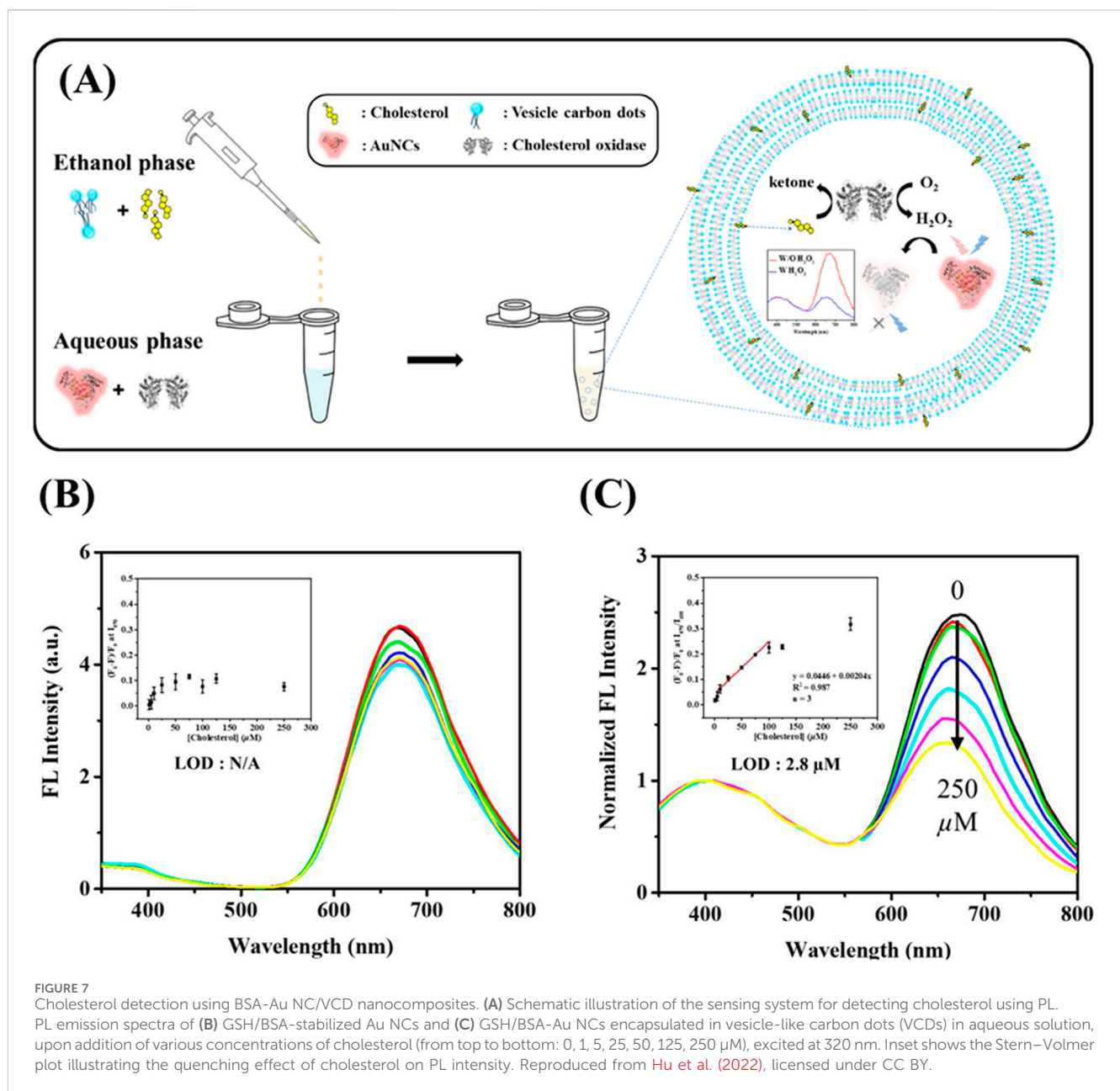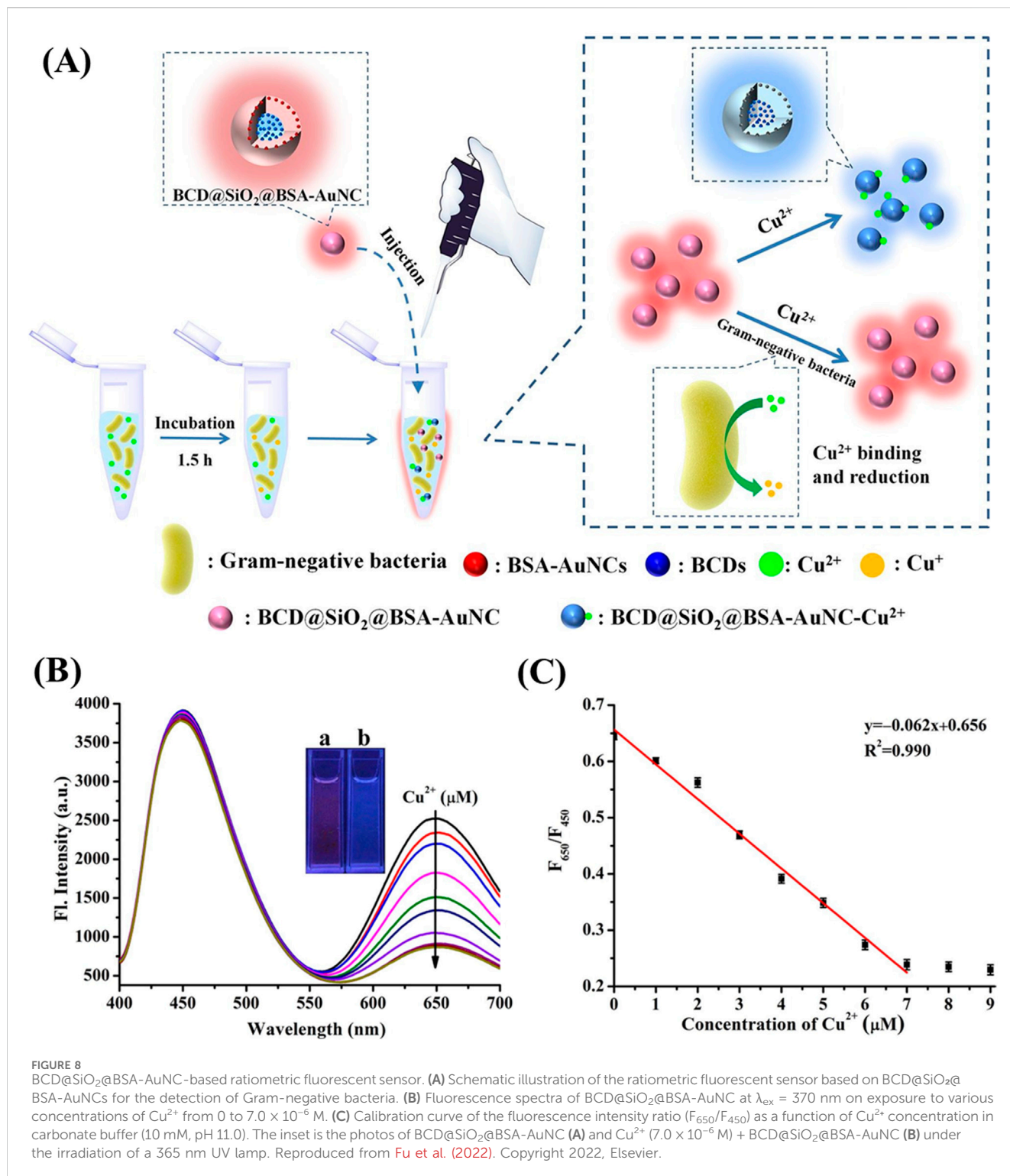
FIGURE 7
Cholesterol detection using BSA-Au NC/VCD nanocomposites. **(A)** Schematic illustration of the sensing system for detecting cholesterol using PL.
PL emission spectra of **(B)** GSH/BSA-stabilized Au NCs and **(C)** GSH/BSA-Au NCs encapsulated in vesicle-like carbon dots (VCDs) in aqueous solution,
upon addition of various concentrations of cholesterol (from top to bottom: 0, 1, 5, 25, 50, 125, 250 μM), excited at 320 nm. Inset shows the Stern−Volmer
plot illustrating the quenching effect of cholesterol on PL intensity. Reproduced from Hu et al. (2022), licensed under CC BY.

metals, such as cadmium (Cd) and palladium (Pd), have been explored, their lower PL efficiency and stability compared to Au, Ag and Cu restrict their applicability. To address this, future research could explore alloying metals or incorporating other metal ions to improve PL properties and extend MNC functionality. Expanding the range of metal cores will be crucial for developing MNCs that exhibit dual-emission properties and broader spectral responses, which are highly desirable for multiplexed sensing and imaging applications.

A pressing challenge is the development of MNCs with PL in the NIR range, particularly in the NIR-II window (1000–1700 nm), which is optimal for deep tissue imaging due to its minimal light scattering and absorption in biological tissues. Currently, protein-templated MNCs lack consistent methods for synthesizing NIR-II

emitting nanoclusters, which limits their use in advanced applications such as deep tumor imaging and precision chemical sensing. Incorporating thiolated ligands or other functional groups into MNCs could be a viable strategy to achieve tunable NIR-II luminescence. Achieving efficient PL in the NIR-II range remains a critical goal for researchers, as this would greatly expand the utility of MNCs in biomedical diagnostics and therapeutic applications.

Future research directions should focus on addressing these limitations and exploring new strategies for MNC synthesis and functionalization. Developing more diverse protein templates, exploring alternative metal cores and achieving tunable NIR-II PL are key areas that will drive the next wave of innovation in MNC-based sensing. Advances in materials science, such as the integration of NCs with stimuli-responsive materials, could lead to

FIGURE 8
BCD@SiO$_2$@BSA-AuNC-based ratiometric fluorescent sensor. **(A)** Schematic illustration of the ratiometric fluorescent sensor based on BCD@SiO$_2$@ BSA-AuNCs for the detection of Gram-negative bacteria. **(B)** Fluorescence spectra of BCD@SiO$_2$@BSA-AuNC at λ_{ex} = 370 nm on exposure to various concentrations of Cu^{2+} from 0 to 7.0 × 10^{-6} M. **(C)** Calibration curve of the fluorescence intensity ratio (F$_{650}$/F$_{450}$) as a function of Cu^{2+} concentration in carbonate buffer (10 mM, pH 11.0). The inset is the photos of BCD@SiO$_2$@BSA-AuNC **(A)** and Cu^{2+} (7.0 × 10^{-6} M) + BCD@SiO$_2$@BSA-AuNC **(B)** under the irradiation of a 365 nm UV lamp. Reproduced from Fu et al. (2022). Copyright 2022, Elsevier.

highly dynamic and adaptable sensors for real-time monitoring in complex biological environments. Moreover, incorporating machine learning and artificial intelligence into sensor design and data interpretation may open new frontiers in the precision and efficiency of MNC-based diagnostics.

In conclusion, while MNCs have demonstrated great promise in sensing, there are still significant challenges to overcome to fully realize their potential. With continued advancements in MNC design, synthesis techniques, and functionalization strategies, MNCs are poised to become central to future innovations in biosensing, early disease detection, environmental monitoring and therapeutic applications. The development of NIR-II emitting MNCs, in particular, will likely revolutionize deep-tissue imaging and disease treatment,

positioning MNCs as pivotal tools in next-generation sensing and biomedical technologies.

Author contributions

H-WC: Writing–original draft, Writing–review and editing. GD: Writing–original draft. C-CH: Writing–review and editing. AA: Writing–original draft, Writing–review and editing.

Funding

Conflict of interest

The authors declare that the research was conducted in the absence of any commercial or financial relationships that could be construed as a potential conflict of interest.

Generative AI statement

The author(s) declare that no Generative AI was used in the creation of this manuscript.

Publisher's note

All claims expressed in this article are solely those of the authors and do not necessarily represent those of their affiliated organizations, or those of the publisher, the editors and the reviewers. Any product that may be evaluated in this article, or claim that may be made by its manufacturer, is not guaranteed or endorsed by the publisher.

References

Aikens, C. M., and Jarrold, C. C. (2023). Virtual issue on experiment–theory synergies in the study of metal and metal-containing clusters. *J. Phys. Chem. A* 127, 3–5. doi:10.1021/acs.jpca.2c08524

Aires, A., Lopez-Martinez, E., and Cortajarena, A. L. (2018). Sensors based on metal nanoclusters stabilized on designed proteins. *Biosensors* 8, 110. doi:10.3390/bios8040110

Akyüz, E., Şen, F. B., Bener, M., Başkan, K. S., and Apak, R. (2020). A novel gold nanocluster–based fluorometric biosensor for measuring prooxidant activity with a large Stokes shift. *Talanta* 208, 120425. doi:10.1016/j.talanta.2019.120425

Aparna, A., Sreehari, H., Chandran, A., Anjali, K. P., Alex, A. M., Anuvinda, P., et al. (2022). Ligand-protected nanoclusters and their role in agriculture, sensingand allied applications. *Talanta* 239, 123134. doi:10.1016/j.talanta.2021.123134

Brocha Silalahi, R. P., Chiu, T.-H., Kao, J.-H., Wu, C.-Y., Yin, C.-W., Liu, Y.-C., et al. (2021). Reactivities of interstitial hydrides in a Cu11 template: en route to bimetallic clusters. *Inorg. Chem.* 60, 10799–10807. doi:10.1021/acs.inorgchem.1c01489

Casteleiro, B., Martinho, J. M. G., and Farinha, J. P. S. (2021). Encapsulation of gold nanoclusters: stabilization and more. *Nanoscale* 13, 17199–17217. doi:10.1039/D1NR04939A

Chakraborty, I., and Parak, W. J. (2019). Protein-induced shape control of noble metal nanoparticles. *Adv. Mat. Interfaces* 6, 1801407. doi:10.1002/admi.201801407

Chakraborty, S., and Mukherjee, S. (2022). Effects of protecting groups on luminescent metal nanoclusters: spectroscopic signatures and applications. *Chem. Commun.* 58, 29–47. doi:10.1039/D1CC05396E

Chang, X., Gao, P., Li, Q., Liu, H., Hou, H., Wu, S., et al. (2021). Fluorescent papain-encapsulated platinum nanoclusters for sensing lysozyme in biofluid and gram-positive bacterial identification. *Sens. Actuators B Chem.* 345, 130363. doi:10.1016/j.snb.2021.130363

Chen, M., Ning, Z., Ge, X., Yang, E., Sun, Q., Yin, F., et al. (2023). Ligands engineering of gold nanoclusters with enhanced photoluminescence for deceptive information encryption and glutathione detection. *Biosens. Bioelectron.* 219, 114805. doi:10.1016/j.bios.2022.114805

Chen, P.-C., Chiang, C.-K., and Chang, H.-T. (2013). Synthesis of fluorescent BSA–Au NCs for the detection of Hg^{2+} ions. *J. Nanopart. Res.* 15, 1336. doi:10.1007/s11051-012-1336-0

Chen, P.-C., Li, Y.-C., Ma, J.-Y., Huang, J.-Y., Chen, C.-F., and Chang, H.-T. (2016). Size-tunable copper nanocluster aggregates and their application in hydrogen sulfide sensing on paper-based devices. *Sci. Rep.* 6, 24882. doi:10.1038/srep24882

Chen, T., Lin, H., Cao, Y., Yao, Q., and Xie, J. (2022). Interactions of metal nanoclusters with light: fundamentals and applications. *Adv. Mat.* 34, 2103918. doi:10.1002/adma.202103918

Chen, X., Wang, T., Le, W., Huang, X., Gao, M., Chen, Q., et al. (2020). Smart sorting of tumor phenotype with versatile fluorescent Ag nanoclusters by sensing specific reactive oxygen species. *Theranostics* 10, 3430–3450. doi:10.7150/thno.38422

Chen, Y.-C., Wang, C.-W., Lee, J. D., Chen, P.-C., and Chang, H.-T. (2016). Control of the fluorescence of DNA-templated silver nanoclusters by adenosine triphosphate and mercury(II). *J. Chin. Chem. Soc.* 64, 8–16. doi:10.1002/jccs.201600246

Chen, Y.-N., Chen, P.-C., Wang, C.-W., Lin, Y.-S., Ou, C.-M., Ho, L.-C., et al. (2014). One-pot synthesis of fluorescent BSA–Ce/Au nanoclusters as ratiometric pH probes. *Chem. Commun.* 50, 8571–8574. doi:10.1039/C4CC03949A

Chen, Y.-W., Periasamy, A. P., Chen, C.-F., and Chang, H.-T. (2019). Quantification of glucose via *in situ* growth of Cu2O/Ag nanoparticles. *Sens. Actuators B* 285, 224–231. doi:10.1016/j.snb.2019.01.050

Cheng, Y., Zhao, Y., Yuan, H., Zhou, H., Xu, J., Chen, X., et al. (2023). Bovine serum albumin protected Cd8 nanoclusters as efficient two-photon absorbers for near-infrared excited fluorescence imaging of intracellular pH. *Sens. Actuators B* 394, 134427. doi:10.1016/j.snb.2023.134427

Cun, X., Jansman, M. M. T., Liu, X., Boureau, V., Thulstrup, P. W., and Hosta-Rigau, L. (2023). Hemoglobin-stabilized gold nanoclusters displaying oxygen transport ability, self-antioxidation, auto-fluorescence propertiesand long-term storage potential. *RSC Adv.* 13, 15540–15553. doi:10.1039/D3RA00689A

Czyżowska, A., Barbasz, A., Szyk-Warszyńska, L., Oćwieja, M., Csapó, E., and Ungor, D. (2021). The surface-dependent biological effect of protein-gold nanoclusters on human immune system mimetic cells. *Colloids Surf. A* 620, 126569. doi:10.1016/j.colsurfa.2021.126569

Deng, H.-H., Deng, Q., Li, K.-L., Zhuang, Q.-Q., Zhuang, Y.-B., Peng, H.-P., et al. (2020). Fluorescent gold nanocluster-based sensor for detection of alkaline phosphatase in human osteosarcoma cells. *Spectrochim. Acta A Mol. Biomol. Spectrosc.* 229, 117875. doi:10.1016/j.saa.2019.117875

Ding, S., Liu, C., Fu, D., Shi, G., and Zhu, A. (2020). Coordination of ligand-protected metal nanoclusters and glass nanopipettes: conversion of a liquid-phase fluorometric assay into an enhanced nanopore analysis. *Anal. Chem.* 93, 1779–1785. doi:10.1021/acs.analchem.0c04620

Dong, W., Yu, J., Gong, X., Liang, W., Fan, L., and Dong, C. (2021). A turn-off-on near-infrared photoluminescence sensor for sequential detection of Fe^{3+} and ascorbic acid based on glutathione-capped gold nanoclusters. *Spectrochimica Acta Part A Mol. Biomol. Spectrosc.* 247, 119085. doi:10.1016/j.saa.2020.119085

Duan, Y., Duan, R., Liu, R., Guan, M., Chen, W., Ma, J., et al. (2018). Chitosan-stabilized self-assembled fluorescent gold nanoclusters for cell imaging and biodistribution *in vivo*. *ACS Biomater. Sci. Eng.* 4, 1055–1063. doi:10.1021/acsbiomaterials.7b00975

Ebina, A., Hossain, S., Horihata, H., Ozaki, S., Kato, S., Kawawaki, T., et al. (2020). One-two-and three-dimensional self-assembly of atomically precise metal nanoclusters. *Nanomaterials* 10, 1105. doi:10.3390/nano10061105

Fang, J., Li, J., Zhang, B., Yuan, X., Asakura, H., Tanaka, T., et al. (2015). The support effect on the size and catalytic activity of thiolated Au25 nanoclusters as precatalysts. *Nanoscale* 7, 6325–6333. doi:10.1039/c5nr00549c

Fereja, S. L., Li, P., Guo, J., Fang, Z., Zhang, Z., Zhuang, Z., et al. (2021). Silver-enhanced fluorescence of bimetallic Au/Ag nanoclusters as ultrasensitive sensing probe for the detection of folic acid. *Talanta* 233, 122469. doi:10.1016/j.talanta.2021.122469

Fu, L., Chen, Q., and Jia, L. (2022). Carbon dots and gold nanoclusters assisted construction of a ratiometric fluorescent biosensor for detection of Gram-negative bacteria. *Food Chem.* 374, 131750. doi:10.1016/j.foodchem.2021.131750

Guo, Y., Amunyela, H. T., Cheng, Y., Xie, Y., Yu, H., Yao, W., et al. (2021). Natural protein-templated fluorescent gold nanoclusters: syntheses and applications. *Food Chem.* 335, 127657. doi:10.1016/j.foodchem.2020.127657

Guo, Y., Han, Y., and Chen, C. (2022). Chiral nanocluster complexes formed by host–guest interaction between enantiomeric 2,6-helic[6]arenes and silver cluster Ag20: emission enhancement and chirality transfer. *Molecules* 27, 3932. doi:10.3390/molecules27123932

Häkkinen, H. (2012). The gold–sulfur interface at the nanoscale. *Nat. Chem.* 4, 443–455. doi:10.1038/nchem.1352

Hossain, S., Imai, Y., Motohashi, Y., Chen, Z., Suzuki, D., Suzuki, T., et al. (2020). Understanding and designing one-dimensional assemblies of ligand-protected metal nanoclusters. *Mat. Horiz.* 7, 796–803. doi:10.1039/C9MH01691K

Hsu, Y.-C., Hung, M.-J., Chen, Y.-A., Wang, T.-F., Ou, Y.-R., and Chen, S.-H. (2019). Identifying reducing and capping sites of protein-encapsulated gold nanoclusters. *Molecules* 24, 1630. doi:10.3390/molecules24081630

Hu, S.-R., Yang, C.-R., Huang, Y.-F., Huang, C.-C., Chen, Y.-L., and Chang, H.-T. (2022). Ratiometric fluorescence probe of vesicle-like carbon dots and gold clusters for quantitation of cholesterol. *Chemosensors* 10, 160. doi:10.3390/chemosensors10050160

Jin, L., Shi, L., Shi, W., Meng, Z., Shang, L., and Shen, Y. (2019). Fluorescence lifetime-based pH sensing by platinum nanoclusters. *Analyst* 144, 3533–3538. doi:10.1039/C9AN00061E

Jin, R. (2015). Atomically precise metal nanoclusters: stable sizes and optical properties. *Nanoscale* 7, 1549–1565. doi:10.1039/C4NR05794E

Jin, R., Li, G., Sharma, S., Li, Y., and Du, X. (2020). Toward active-site tailoring in heterogeneous catalysis by atomically precise metal nanoclusters with crystallographic structures. *Chem. Rev.* 121, 567–648. doi:10.1021/acs.chemrev.0c00495

Kailasa, S. K., Borse, S., Koduru, J. R., and Murthy, Z. (2021). Biomolecules as promising ligands in the synthesis of metal nanoclusters: sensing, bioimaging and catalytic applications. *Trac. Trends Environ. Anal. Chem.* 32, e00140. doi:10.1016/j.teac.2021.e00140

Kang, X., Wang, S., Song, Y., Jin, S., Sun, G., Yu, H., et al. (2016). Bimetallic Au2Cu6 nanoclusters: strong luminescence induced by the aggregation of copper(I) complexes with gold(0) species. *Angew. Chem. Int. Ed.* 55, 3611–3614. doi:10.1002/anie.201600241

Kang, X., and Zhu, M. (2019). Metal nanoclusters stabilized by selenol ligands. *Small* 15, 1902703. doi:10.1002/smll.201902703

Khataee, A., Jalili, R., Dastborhan, M., Karimi, A., and Azar, A. E. F. (2020). Ratiometric visual detection of tetracycline residues in milk by framework-enhanced fluorescence of gold and copper nanoclusters. *Spectrochim. Acta A Mol. Biomol. Spectrosc.* 242, 118715. doi:10.1016/j.saa.2020.118715

Koga, H., Sakata, K., Ato, Y., Hayashi, A., Tada, K., and Okumura, M. (2016). Advances in polymer-stabilized Au nano-cluster catalysis: interplay of theoretical calculations and experiments. *Chin. J. Catal.* 37, 1588–1593. doi:10.1016/S1872-2067(16)62463-4

Kolay, S., Bain, D., Maity, S., Devi, A., Patra, A., and Antoine, R. (2022). Self-assembled metal nanoclusters: driving forces and structural correlation with optical properties. *Nanomaterials* 12, 544. doi:10.3390/nano12030544

Kong, X.-J., Tian, J.-X., Fang, Y.-Z., Chen, T.-L., Yu, R., He, J.-Y., et al. (2022). Terbium metal-organic framework/bovine serum albumin capped gold nanoclusters-based dual-emission reverse change ratio fluorescence nanoplatform for fluorimetric and colorimetric sensing of heparin and chondroitin sulfate. *Sens. Actuators B Chem.* 356, 131331. doi:10.1016/j.snb.2021.131331

Lettieri, M., Palladino, P., Scarano, S., and Minunni, M. (2021). Protein-templated copper nanoclusters for fluorimetric determination of human serum albumin. *Microchim. Acta* 188, 116–119. doi:10.1007/s00604-021-04764-7

Li, C., and Wei, C. (2017). DNA-templated silver nanocluster as a label-free fluorescent probe for the highly sensitive and selective detection of mercury ions. *Sens. Actuators B Chem.* 242, 563–568. doi:10.1016/j.snb.2016.11.091

Li, J.-J., Qiao, D., Zhao, J., Weng, G.-J., Zhu, J., and Zhao, J.-W. (2019). Ratiometric fluorescence detection of Hg^{2+} and Fe^{3+} based on BSA-protected Au/Ag nanoclusters and His-stabilized Au nanoclusters. *Methods Appl. Fluoresc.* 7, 045001. doi:10.1088/2050-6120/ab34be

Li, P., Xie, Z., Zhuang, L., Deng, L., and Huang, J. (2023). DNA-templated copper nanocluster: a robust and universal fluorescence switch for bleomycin assay. *Int. J. Biol. Macromol.* 234, 123756. doi:10.1016/j.ijbiomac.2023.123756

Li, X., Luo, J., Jiang, X., Yang, M., and Rasooly, A. (2021). Gold nanocluster-europium (III) ratiometric fluorescence assay for dipicolinic acid. *Microchim. Acta* 188, 26–28. doi:10.1007/s00604-020-04667-z

Li, Y., Zhou, M., and Jin, R. (2021). Programmable metal nanoclusters with atomic precision. *Adv. Mat.* 33, 2006591. doi:10.1002/adma.202006591

Lin, H., Song, X., Huang Chai, O. J., Yao, Q., Yang, H., and Xie, J. (2024). Photoluminescent characterization of metal nanoclusters: basic parameters, methodsand applications. *Adv. Mater* 36, 2401002. doi:10.1002/adma.202401002

Lin, Y.-F., Yang, C.-R., Huang, Y.-F., and Chang, H.-T. (2022). Fluorescent carbon dots and noble metal nanoclusters for sensing applications: minireview. *J. Chin. Chem. Soc.* 69, 1200–1209. doi:10.1002/jccs.202200150

Lin, Y.-S., Chuang, L.-W., Wu, B.-Y., Lin, Y.-H., and Chang, H.-T. (2021a). Polymer/glutathione Au nanoclusters for detection of sulfides. *Sens. Actuators B* 333, 129356. doi:10.1016/j.snb.2020.129356

Lin, Y.-S., Lin, Y.-F., Nain, A., Huang, Y.-F., and Chang, H.-T. (2021b). A critical review of copper nanoclusters for monitoring of water quality. *Sens. Actuators Rep.* 3, 100026. doi:10.1016/j.snr.2021.100026

Lipok, M., Obstarczyk, P., Parzyszek, S., Wang, Y., Bagiński, M., Bürgi, T., et al. (2023). Circularly polarized luminescence from atomically precise gold nanoclusters helically assembled by liquid-crystal template. *Adv. Opt. Mat.* 11, 2201984. doi:10.1002/adom.202201984

Liu, R., Duan, S., Bao, L., Wu, Z., Zhou, J., and Yu, R. (2020). Photonic crystal enhanced gold-silver nanoclusters photoluminescent sensor for Hg^{2+} ion. *Anal. Chim. Acta* 1114, 50–57. doi:10.1016/j.aca.2020.04.011

Liu, Z., Luo, L., and Jin, R. (2024). Visible to NIR-II photoluminescence of atomically precise gold nanoclusters. *Angew. Chem. Int. Ed.* 36, 2309073. doi:10.1002/adma.202309073

López-Domene, R., Vázquez-Díaz, S., Modin, E., Beloqui, A., and Cortajarena, A. L. (2023). An emerging nanozyme class for à la carte enzymatic-like activities based on protein-metal nanocluster hybrids. *Adv. Funct. Mat.* 33, 2301131. doi:10.1002/adfm.202301131

Luo, Z., Yuan, X., Yu, Y., Zhang, Q., Leong, D. T., Lee, J. Y., et al. (2012). From aggregation-induced emission of Au(I)–thiolate complexes to ultrabright Au(0) @Au(I)–thiolate core–shell nanoclusters. *J. Am. Chem. Soc.* 134, 16662–16670. doi:10.1021/ja306199p

Mathew, M. S., Krishnan, G., Mathews, A. A., Sunil, K., Mathew, L., Antoine, R., et al. (2023). Recent progress on ligand-protected metal nanoclusters in photocatalysis. *Nanomaterials* 13, 1874. doi:10.3390/nano13121874

Matus, M. F., and Häkkinen, H. (2023). Understanding ligand-protected noble metal nanoclusters at work. *Nat. Rev. Mat.* 8, 372–389. doi:10.1038/s41578-023-00537-1

Mitsui, M., Arima, D., Kobayashi, Y., Lee, E., and Niihori, Y. (2022). On the origin of photoluminescence enhancement in biicosahedral Ag_xAu_{25-x} nanoclusters ($x = 0$–13) and their application to triplet–triplet annihilation photon upconversion. *Adv. Opt. Mat.* 10, 2200864. doi:10.1002/adom.202200864

Miyamura, H., Yasukawa, T., and Kobayashi, S. (2014). Preparation of polymer incarcerated gold nanocluster catalysts (PI-Au) and their application to aerobic oxidation reactions of boronic acids, alcoholsand silyl enol ethers. *Tetrahedron* 70, 6039–6049. doi:10.1016/j.tet.2014.05.014

Nain, A., Tseng, Y.-T., Lin, Y.-S., Wei, S.-C., Mandal, R. P., Unnikrishnan, B., et al. (2020). Tuning the photoluminescence of metal nanoclusters for selective detection of multiple heavy metal ions. *Sens. Actuators B* 321, 128539. doi:10.1016/j.snb.2020.128539

Nasrollahpour, H., Jurado Sánchez, B., Sillanpää, M., and Moradi, R. (2023). Metal nanoclusters in point-of-care sensing and biosensing applications. *ACS Appl. Nano Mat.* 6, 12609–12672. doi:10.1021/acsanm.3c01569

New, S. Y., Lee, S. T., and Su, X. D. (2016). DNA-templated silver nanoclusters: structural correlation and fluorescence modulation. *Nanoscale* 8, 17729–17746. doi:10.1039/C6NR05872H

O'Neill, P. R., Velazquez, L. R., Dunn, D. G., Gwinn, E. G., and Fygenson, D. K. (2009). Hairpins with poly-C loops stabilize four types of fluorescent Agn. *J. Phys. Chem. C* 113, 4229–4233. doi:10.1021/jp809274m

Panthi, G., and Park, M. (2022). Synthesis of metal nanoclusters and their application in Hg^{2+} ions detection: a review. *J. Hazard. Mat.* 424, 127565. doi:10.1016/j.jhazmat.2021.127565

Paulrajpillai, L. X., Chaudhari, K., Baksi, A., and Pradeep, T. (2012). Protein-protected luminescent noble metal quantum clusters: an emerging trend in atomic cluster nanoscience. *Nano Rev.* 3, 14767. doi:10.3402/nano.v3i0.14767

Pei, G. X., Zhang, L., and Sun, X. (2024). Recent advances of bimetallic nanoclusters with atomic precision for catalytic applications. *Coord. Chem. Rev.* 506, 215692. doi:10.1016/j.ccr.2024.215692

Pyo, K., Thanthirige, V. D., Kwak, K., Pandurangan, P., Ramakrishna, G., and Lee, D. (2015). Ultrabright luminescence from gold nanoclusters: rigidifying the Au(I)-thiolate shell. *J. Am. Chem. Soc.* 137, 8244–8250. doi:10.1021/jacs.5b04210

Qian, S., Wang, Z., Zuo, Z., Wang, X., Wang, Q., and Yuan, X. (2022). Engineering luminescent metal nanoclusters for sensing applications. *Coord. Chem. Rev.* 451, 214268. doi:10.1016/j.ccr.2021.214268

Qiao, Z., Yan, Y., and Bi, S. (2022). Three-dimensional DNA structures *in situ* decorated with metal nanoclusters for dual-mode biosensing of glucose. *Sens. Actuators B* 352, 131073. doi:10.1016/j.snb.2021.131073

Qiao, Z., Zhang, J., Hai, X., Yan, Y., Song, W., and Bi, S. (2021). Recent advances in templated synthesis of metal nanoclusters and their applications in biosensing,

bioimaging and theranostics. *Biosens. Bioelectron.* 176, 112898. doi:10.1016/j.bios.2020. 112898

Romeo, M. V., Lopez-Martinez, E., Berganza-Granda, J., Goni-de-Cerio, F., and Cortajarena, A. L. (2021). Biomarker sensing platforms based on fluorescent metal nanoclusters. *Nanoscale Adv.* 3, 1331–1341. doi:10.1039/D0NA00796J

Sam, S., Swathy, S., and Kumar, K. G. (2024). Lysozyme functionalized silver nanoclusters as a dual channel optical sensor for the effective determination of glutathione. *Talanta* 277, 126326. doi:10.1016/j.talanta.2024.126326

Sarkar, P., Nandi, N., Barnwal, N., and Sahu, K. (2023). BSA-capped dual-emissive silver nanoclusters for detection of IO₄⁻ and Cu²⁺ ions. *ACS Appl. Nano Mat.* 6, 15851–15859. doi:10.1021/acsanm.3c02752

Sebastian, A., Aarya, Sarangi, B. R., and Sen Mojumdar, S. (2023). Lysozyme protected copper nano-cluster: a photo-switch for the selective sensing of Fe²⁺. *J. Photochem. Photobiol. A Chem.* 436, 114378. doi:10.1016/j.jphotochem.2022.114378

Shen, J., Xiao, Q., Sun, P., Feng, J., Xin, X., Yu, Y., et al. (2021). Self-assembled chiral phosphorescent microflowers from Au nanoclusters with dual-mode pH sensing and information encryption. *ACS Nano* 15, 4947–4955. doi:10.1021/acsnano.0c09766

Sinha-Roy, R., García-González, P., López-Lozano, X., and Weissker, H.-C. (2023). Visualizing screening in noble-metal clusters: static vs. dynamic. *Phys. Chem. Chem. Phys.* 25, 2075–2083. doi:10.1039/D2CP04316E

Song, C., Xu, J., Chen, Y., Zhang, L., Lu, Y., and Qing, Z. (2019). DNA-templated fluorescent nanoclusters for metal ions detection. *Molecules* 24, 4189. doi:10.3390/molecules24224189

Song, Y., Li, Y., Zhou, M., Liu, X., Li, H., Wang, H., et al. (2021). Ultrabright Au@Cu14 nanoclusters: 71.3% phosphorescence quantum yield in non-degassed solution at room temperature. *Sci. Adv.* 7, eabd2091. doi:10.1126/sciadv.abd2091

Sun, H., Qing, T., He, X., Shangguan, J., Jia, R., Bu, H., et al. (2019). Rapid synthesis of Au/Ag bimetallic nanoclusters with highly biochemical stability and its applications for temperature and ratiometric pH sensing. *Anal. Chim. Acta* 1070, 88–96. doi:10.1016/j.aca.2019.04.029

Suo, Z., Hou, X., Hu, Z., Liu, Y., Xing, F., and Feng, L. (2019). Fibrinogen-templated gold nanoclusters for fluorometric determination of cysteine and mercury (II). *Microchim. Acta* 186, 799–9. doi:10.1007/s00604-019-3919-2

Tan, S. C. L., He, Z., Wang, G., Yu, Y., and Yang, L. (2023). Protein-templated metal nanoclusters: molecular-like hybrids for biosensing, diagnosticsand pharmaceutics. *Molecules* 28, 5531. doi:10.3390/molecules28145531

Tang, X., Lu, M., Wang, J., Man, S., Peng, W., and Ma, L. (2024). Recent advances of DNA-templated metal nanoclusters for food safety detection: from synthesis, applications, challengesand beyond. *J. Agric. Food Chem.* 72, 5542–5554. doi:10.1021/acs.jafc.3c09621

Thakran, A., Nain, A., Kataria, M., Paul Inbaraj, C. R., Lin, H.-Y., Lin, H.-I., et al. (2021). Highly efficient photodetection in metal nanocluster/graphene heterojunctions. *ACS Photonics* 8, 2955–2965. doi:10.1021/acsphotonics.1c00885

Tseng, Y.-T., Chang, H.-Y., Harroun, S. G., Wu, C.-W., Wei, S.-C., Yuan, Z., et al. (2018). Self-assembled chiral gold supramolecules with efficient laser absorption for enantiospecific recognition of carnitine. *Anal. Chem.* 90, 7283–7291. doi:10.1021/acs.analchem.8b00490

van de Looij, S. M., Hebels, E. R., Viola, M., Hembury, M., Oliveira, S., and Vermonden, T. (2021). Gold nanoclusters: imaging, therapyand theranostic roles in biomedical applications. *Bioconjugate Chem.* 33, 4–23. doi:10.1021/acs.bioconjchem.1c00475

Vilar-Vidal, N., Rivas, J., and Lopez-Quintela, M. A. (2012). Size dependent catalytic activity of reusable subnanometer copper (0) clusters. *ACS Catal.* 2, 1693–1697. doi:10.1021/cs300355n

Voet, A. R., and Tame, J. R. (2017). Protein-templated synthesis of metal-based nanomaterials. *Curr. Opin. Biotechnol.* 46, 14–19. doi:10.1016/j.copbio.2016.10.015

Wang, C. C., Wu, S. M., Li, H. W., and Chang, H. T. (2016). Biomedical applications of DNA-conjugated gold nanoparticles. *ChemBioChem* 17, 1052–1062. doi:10.1002/cbic.201600014

Wang, C.-W., Chen, Y.-N., Wu, B.-Y., Lee, C.-K., Chen, Y.-C., Huang, Y.-H., et al. (2016). Sensitive detection of cyanide using bovine serum albumin-stabilized cerium/gold nanoclusters. *Anal. Bioanal. Chem.* 408, 287–294. doi:10.1007/s00216-015-9104-5

Wang, H.-B., Bai, H.-Y., Dong, G.-L., and Liu, Y.-M. (2019). DNA-templated Au nanoclusters coupled with proximity-dependent hybridization and guanine-rich DNA induced quenching: a sensitive fluorescent biosensing platform for DNA detection. *Nanoscale Adv.* 1, 1482–1488. doi:10.1039/C8NA00278A

Wang, M., Li, H., Wang, Y., Hu, X., Fang, S., Ma, H., et al. (2023). Spatial confinement-enhanced electrochemiluminescence of gold nanoclusters in chitosan nanogels and its application for ultrasensitive detection of aflatoxin B1. *J. Electroanal. Chem.* 943, 117595. doi:10.1016/j.jelechem.2023.117595

Wang, S., Meng, X., Das, A., Li, T., Song, Y., Cao, T., et al. (2014). A 200-fold quantum yield boost in the photoluminescence of silver-doped AgxAu25-x nanoclusters: the 13th silver atom matters. *Angew. Chem. Int. Ed.* 53, 2376–2380. doi:10.1002/anie.201307480

Wei, S., Li, Y., Liang, H., Yen, Y., Lin, Y., and Chang, H. (2022). Photoluminescent carbon nanomaterials for sensing of illicit drugs: focus. *Anal. Sci.* 38, 247–260. doi:10.2116/analsci.21SAR06

Wen, Q.-L., Peng, J., Liu, A.-Y., Hu, Y.-L., Wang, J., Ling, J., et al. (2020). Fluorescent silver nanoclusters stabilized in guanine-enhanced DNA hybridization for recognizing different small biological molecules. *J. Lumin.* 221, 117038. doi:10.1016/j.jlumin.2020.117038

Wong, X. Y., Quesada-González, D., Manickam, S., New, S. Y., Muthoosamy, K., and Merkoçi, A. (2021). Integrating gold nanoclusters, folic acidand reduced graphene oxide for nanosensing of glutathione based on "turn-off" fluorescence. *Sci. Rep.* 11, 2375. doi:10.1038/s41598-021-81677-8

Wu, B.-Y., Wang, C.-W., Chen, P.-C., and Chang, H.-T. (2017). Glutathione assisted preparation of gold nanoclusters using minimum amount of protein. *Sens. Actuators B Chem.* 238, 1258–1265. doi:10.1016/j.snb.2016.09.071

Wu, X., Wu, P., Gu, M., and Xue, J. (2020). Ratiometric fluorescent probe based on AuNCs induced AIE for quantification and visual sensing of glucose. *Anal. Chim. Acta* 1104, 140–146. doi:10.1016/j.aca.2020.01.004

Xiao, W., Zhi, D., Pan, Q., Liang, Y., Zhou, F., and Chen, Z. (2020). A ratiometric bilirubin sensor based on a fluorescent gold nanocluster film with dual emissions. *Anal. Methods* 12, 5691–5698. doi:10.1039/D0AY01781G

Xiao, Y., Wu, Z., Yao, Q., and Xie, J. (2021). Luminescent metal nanoclusters: biosensing strategies and bioimaging applications. *Aggregate* 2, 114–132. doi:10.1002/agt2.11

Xie, J., Zheng, Y., and Ying, J. Y. (2009). Protein-directed synthesis of highly fluorescent gold nanoclusters. *J. Am. Chem. Soc.* 131, 888–889. doi:10.1021/ja806804u

Xu, D., Lin, Q., and Chang, H.-T. (2019). Chiral Ag and Au nanomaterials based optical approaches for analytical applications. *Part. Part. Syst. Charact.* 36, 1800552. doi:10.1002/ppsc.201800552

Xu, F., Qing, T., and Qing, Z. (2021). DNA-coded metal nano-fluorophores: preparation, properties and applications in biosensing and bioimaging. *Nano Today* 36, 101021. doi:10.1016/j.nantod.2020.101021

Xu, M.-M., Jia, T.-T., Li, B., Ma, W., Chen, X., Zhao, X., et al. (2020). Tuning the properties of atomically precise gold nanoclusters for biolabeling and drug delivery. *Chem. Commun.* 56, 8766–8769. doi:10.1039/D0CC03498C

Xu, Y., Sherwood, J., Qin, Y., Crowley, D., Bonizzoni, M., and Bao, Y. (2014). The role of protein characteristics in the formation and fluorescence of Au nanoclusters. *Nanoscale* 6, 1515–1524. doi:10.1039/C3NR06040C

Yang, C., Deng, H., He, J., Zhang, X., Gao, J., Shang, X., et al. (2022). Amplifiable ratiometric fluorescence biosensing of nanosilver multiclusters populated in three-way-junction DNA branches. *Biosens. Bioelectron.* 199, 113871. doi:10.1016/j.bios.2021.113871

Yang, M., Zhu, L., Yang, W., and Xu, W. (2023). Nucleic acid-templated silver nanoclusters: a review of structures, propertiesand biosensing applications. *Coord. Chem. Rev.* 491, 215247. doi:10.1016/j.ccr.2023.215247

Yang, T.-Q., Peng, B., Shan, B.-Q., Zong, Y.-X., Jiang, J.-G., Wu, P., et al. (2020). Origin of the photoluminescence of metal nanoclusters: from metal-centered emission to ligand-centered emission. *Nanomaterials* 10, 261. doi:10.3390/nano10020261

Yarramala, D. S., Baksi, A., Pradeep, T., and Rao, C. P. (2017). Green synthesis of protein-protected photoluminescent gold nanoclusters (AuNCs): reducing the size of AuNCs by partially occupying the Ca²⁺ site by La³⁺ in apo-α-lactalbumin. *ACS Sustain. Chem. Eng.* 5, 6064–6069. doi:10.1021/acssuschemeng.7b00958

Yen, Y.-T., Chen, T.-Y., Chen, C.-Y., Chang, C.-L., Chyueh, S.-C., and Chang, H.-T. (2019). A photoluminescent colorimetric probe of bovine serum albumin-stabilized gold nanoclusters for new psychoactive substances: cathinone drugs in seized street samples. *Sensors* 19, 3554. doi:10.3390/s19163554

Yen, Y.-T., Lin, Y.-S., Chang, Y.-J., Li, M.-T., Chyueh, S.-C., and Chang, H.-T. (2022). Nanomaterial-based sensor arrays with deep learning for screening of illicit drugs. *Adv. Mat. Technol.* 7, 2200243. doi:10.1002/admt.202200243

Yu, Q., Gao, P., Zhang, K. Y., Tong, X., Yang, H., Liu, S., et al. (2017). Luminescent gold nanocluster-based sensing platform for accurate H₂S detection *in vitro* and *in vivo* with improved anti-interference. *Light Sci. Appl.* 6, e17107. doi:10.1038/lsa.2017.107

Yu, Y., Di Lee, W., and Tan, Y. N. (2020). Protein-protected gold/silver alloy nanoclusters in metal-enhanced singlet oxygen generation and their correlation with photoluminescence. *Mat. Sci. Eng. C* 109, 110525. doi:10.1016/j.msec.2019.110525

Yuan, H., Lin, J.-H., Dong, Z.-S., Chen, W.-T., Chan, Y. K., Yeh, Y.-C., et al. (2022). Detection of pathogens using graphene quantum dots and gold nanoclusters on paper-based analytical devices. *Sens. Actuators B Chem.* 363, 131824. doi:10.1016/j.snb.2022.131824

Yuan, X., Chng, L. L., Yang, J., and Ying, J. Y. (2020). Miscible-solvent-assisted two-phase synthesis of monolayer-ligand-protected metal nanoclusters with various sizes. *Adv. Mat.* 32, 1906063. doi:10.1002/adma.201906063

Zaleska-Medynska, A., Marchelek, M., Diak, M., and Grabowska, E. (2016). Noble metal-based bimetallic nanoparticles: the effect of the structure on the optical, catalyticand photocatalytic properties. *Adv. Colloid Interface Sci.* 229, 80–107. doi:10.1016/j.cis.2015.12.008

Zare, I., Chevrier, D. M., Cifuentes-Rius, A., Moradi, N., Xianyu, Y., Ghosh, S., et al. (2021). Protein-protected metal nanoclusters as diagnostic and therapeutic platforms for biomedical applications. *Mat. Today* 66, 159–193. doi:10.1016/j.mattod.2020.10.027

Zhang, B., Chen, J., Cao, Y., Chai, O. J. H., and Xie, J. (2021). Ligand design in ligand-protected gold nanoclusters. *Small* 17, 2004381. doi:10.1002/smll.202004381

Zhang, X., Qian, Y., Ma, X., Xia, M., Li, S., and Zhang, Y. (2018). Thiolated DNA-templated silver nanoclusters with strong fluorescence emission and a long shelf-life. *Nanoscale* 10, 76–81. doi:10.1039/C7NR06358J

Zhang, Y., Xu, H., Yang, Y., Zhu, F., Pu, Y., You, X., et al. (2021). Efficient fluorescence resonance energy transfer-based ratiometric fluorescent probe for detection of dopamine using a dual-emission carbon dot-gold nanocluster nanohybrid. *J. Photochem. Photobiol. A Chem.* 411, 113195. doi:10.1016/j.jphotochem.2021.113195

Zhang, Z., Liu, T., Wang, S., Ma, J., Zhou, T., Wang, F., et al. (2019). DNA-templated gold nanocluster as a novel fluorometric sensor for glutathione determination. *J. Photochem. Photobiol. A Chem.* 370, 89–93. doi:10.1016/j.jphotochem.2018.10.021

Zhou, W., Fang, Y., Ren, J., and Dong, S. (2019). DNA-templated silver and silver-based bimetallic clusters with remarkable and sequence-related catalytic activity toward 4-nitrophenol reduction. *Chem. Commun.* 55, 373–376. doi:10.1039/C8CC08810A

Zhu, Y., Li, W., Ju, C., Gong, X., Song, W., Zhao, Y., et al. (2019). Selective detection of glutathione based on the recovered fluorescence of BSA-AuNCs/Cu^{2+} system. *Micro and Nano Lett.* 14, 952–956. doi:10.1049/mnl.2018.5772